Optimal Event-Triggered Consensus for Multiagent Systems via Game-Theoretic Approaches

Wentao Wu, *Member, IEEE*, Lei Xu, *Member, IEEE*, Yibo Zhang, *Member, IEEE*, Weidong Zhang, *Senior Member, IEEE*, and Yang Shi, *Fellow, IEEE*

***Abstract*—This paper investigates the optimal consensus problem for leader-follower multiagent systems (MASs) via event-triggered control. Within a game-theoretic framework, a novel optimal event-triggered consensus scheme is proposed to achieve the dual optimization of control performance and sampling frequency. Given that the impact on system performance, the control input and the event-based sampling error are regarded as two competitive players of the zero-sum game. In the MAS consensus, each agent is to minimize its performance index against the actions of neighboring agents, which can be formulated as the differential graphical game. In the game-theoretic framework, the optimal event-based control law and the optimal event-triggered mechanism are derived by seeking the global Nash equilibrium. Our designed sampling mechanism can not only maximize the interevent interval with respect to the performance index but also guarantee the exclusion of the Zeno behavior. Finally, simulation results are conducted to validate the effectiveness of the proposed optimal event-triggered consensus method.**

***Note to Practitioners*—Consensus control of multiagent systems (MASs) has been of great interest due to extensive engineering applications, such as multivehicle formation, distributed optimization, smart grids, and sensor networks. However, realistic agents are usually only equipped with limited communication capability, which restricts the advancement of the MAS consensus. This paper adopts the game-theoretic approach to develop an optimal event-triggered consensus framework for MASs, where the control input and its sampling error are treated as competing players in a zero-sum game, and policy pairs among neighboring agents are regarded as competing players in a differential graphical game. The Nash equilibrium solution of games establishes the optimal control policy and the maximum triggering threshold, which is used to design the optimal event-triggered mechanism with the maximum sampling interval. Unlike prior event-triggered schemes focused solely on stability, the key feature of the proposed framework is designed under the premise of both stability and optimality, which benefits the balance between control performance and sampling efficiency. The theoretical results and simulations show that the triggering mechanism excludes Zeno behaviors, thereby ensuring practical feasibility for hardware implementations.**

***Index Terms*—Event-triggered mechanism, differential graphical game, multiagent systems, optimal consensus, zero-sum game.**

This work is supported by the National Science and Technology Major Project under Grant 2022ZD0119900, the National Natural Science Foundation of China under Grants U2141234, U24A20260, 52201369, and Hainan Province Science and Technology Special Fund under Grant ZDYF2024GXJS003. (*Corresponding author: Weidong Zhang.*)

W. Wu is with the School of Automation and Intelligent Sensing, Shanghai Jiao Tong University, Shanghai 200240, China, with the Department of Aeronautical and Aviation Engineering, The Hong Kong Polytechnic University, Hong Kong, SAR, China, and also with the Research Centre for Low-Altitude Economy, The Hong Kong Polytechnic University, Hong Kong, SAR, China (e-mail: wtwu95@gmail.com).

W. Zhang is with the School of Automation and Intelligent Sensing, Shanghai Jiao Tong University, Shanghai 200240, China (e-mail: wdzhang@sjtu.edu.cn).

L. Xu is with the Division of Decision and Control Systems, School of Electrical Engineering and Computer Science, KTH Royal Institute of Technology, and also affiliated with Digital Futures, 100 44, Stockholm, Sweden (e-mail: lei5@kth.se).

Y. Zhang is with the Department of Automation, Shanghai University, Shanghai 200444, China (e-mail: ybzhang@shu.edu.cn).

Y. Shi is with the Department of Mechanical Engineering, University of Victoria, Victoria BC V8W 2Y2, Canada (e-mail: yshi@uvic.ca).

I. Introduction

OVER the past decade, coordination of multiagent systems (MASs) has emerged as an research hotspot due to diverse engineering applications like multivehicle formation [1]–[5], distributed optimization [6], [7], smart grids [8], [9], and sensor networks [10], [11]. Consensus control, one core issue of the coordination control, drives states of all agents to reach agreement in practical scenarios, such as synchronizing inter-vehicle spacing and speed in the platoon formation [12], [13] and distributed energy management in smart grids [14]. In reality, constrained communication capabilities of individual agents pose a significant challenge for a central controller, whereas distributed or decentralized controllers provide a more realistic scheme due to no requirement for global information. Therefore, it is challenging but essential to develop novel distributed controllers for MASs.

Due to a pragmatic significance, many profound results about consensus control problem have been reported including academic and engineering fields [15]–[21]. Later on, optimal consensus control has received considerable attention, which is expected to simultaneously obtain better control performance and consensus. Many efforts have been devoted to investigating the optimal consensus problem. In [22], structured quadratic performance indices are derived to achieve the global optimal control of linear MASs with a fixed and directed topology. [23] and [24] further extend the result of [22] to general linear MASs and discrete-time MASs with constrained control inputs. In [25], the linear quadratic regulation is introduced to design the optimal distributed controller for reaching the consensus of quadrotors and mobile robots. Moreover, distributed optimal control method based on date-driven technique [26], model predictive control [27], and dynamic average consensus [28] are developed for MASs. It should be pointed out that practical systems (e.g., autonomous aerial/surface/underwater vehicles) carry usually equipment with limited energy and communication capabilities, which leads to the implementation difficulty of aforementioned optimal consensus methods via continuous communications. Thus, the development of resource-saving controllers is crucial to improving the practicality.

As reviewed in the literature [29], [30], consensus control employ the continuous-time state or output information from neighboring agents, which necessitates continuous consumption of system resources. To mitigate this weakness, the sampled-data control scheme provides a way to reduce resource consumption, which only updates control laws or exchanges information under certain specific conditions. Note that the key step of event-triggered control (ETC) is to develop appropriate event-triggering conditions, also called event-triggered mechanisms (ETMs), for determining sampling instants [31]. A common feature of ETMs lies in the triggering function associated with the sampling error bounded by some state- and/or time-dependent functions. A time-dependent ETM is designed in [32] to bound the measurement error for the asymptotic consensus. Different from time-dependent threshold, [33] derives a state-dependent threshold for the distributed static ETM, which guarantees the positive lower bound on the average interevent interval. In [34] and [35], adaptive technique is employed to the development of ETMs. In [34], an online adaptive parameter is introduced to derive a dynamic triggering function for avoiding continuously monitoring the system state. [35] presents an adaptive ETM capable of achieving event-triggered consensus without any global information of topology graph. In contrast to static ETMs, the dynamic triggering threshold designed in [36] enlarges the inter-sampling interval between consecutive events by introducing an internal variable. In [37], a distributed ETM with a time-varying threshold is designed for leaderless and leader-follower consensuses to reduce the information transmission between agent and its neighbors. To seek a tradeoff between convergence rate and sampling frequency, [38] develops a dynamic triggering function to achieve the designable minimum interevent interval. Other dynamic ETC methods are also investigated, such as distributed dynamic ETC [39] and fully distributed ETC [40], and edge-based triggering mechanisms [41] and [42].

Recalling aforementioned results, these event-triggered consensus methods have developed various triggering functions, which are expected to achieve the largest possible triggering interval on the premise of stability. It is noted that above design schemes can not provide the interval-maximum sampling condition and also oversight the relationship between control performance and sampling frequency. Moreover, individual performance index of all agents leads to the noncooperative feature among them, which concerns the minimization of their own cost functions. However, it is inadequate to solve optimal event-triggered consensus problems with above methods. Therefore, it is challenging but promising to simultaneously take into account noncooperative relationship among agents and co-optimality of both control performance and triggering condition.

Motivated by the above discussions, this paper develops an optimal event-triggered consensus method for leader-follower MASs using game-theoretic approaches. The main contributions are presented as follows.

- In the game-theoretic framework, an optimal event-triggered consensus control method is developed to simultaneously consider the optimalities of control performance and event-triggered mechanism involving two noncooperative game perspectives. With our proposed optimal ETC method, the tradeoff between system performance and sampling frequency is obtained by the global Nash equilibrium seeking.
- Based on the min-max strategy and the zero-sum game approach, the maximum inter-sampling interval with respect to individual performance function is determined, which is employed to derive the optimal event-triggered mechanism. In contrast to the optimal ETC schemes for single agent system in [43] and [44], our designed mechanism is a distributed scheme to reduce information exchanges among agents.
- According to the game algebraic Riccati and Hamilton-Jacobi-Isaacs equations, the optimal control policy and the sampling error are derived to guarantee both the stability of the closed-loop system and the Zeno-free behavior.

The rest of this paper is organized as below. Section II introduces preliminaries and problem formulation. Section III develops the optimal event-triggered consensus control method and gives the stability analysis. Section IV provides the simulation verification. Section V concludes this paper.

II. Preliminaries and Problem Formulation

A. Notations

Let $\mathbb{N}_{>0}$ and $\mathbb{R}_{>0}$ be the sets of positive integers and nonnegative real numbers, respectively. For any $n \in \mathbb{N}_{>0}$, $\mathbf{1}_n$ and $\mathbf{0}_n$ are $n \times 1$ column vectors with all elements equal to one and zero, respectively. $\boldsymbol{I}_n$ and $\mathbf{0}_{n\times n}$ denote the $n \times n$ identity matrix and $n\times n$ matrix with all zeros. For brevity, $\mathbb{I}_{1:n}$ represents a integer set $\{1, ..., n\}$. Denote $\operatorname{col}(\cdot)$ and $\operatorname{diag}(\cdot)$ as the column vector and block-diagonal matrix, sequentially. $\otimes$ is the Kronecker Product. $\|\cdot\|$ stands for the Euclidean norm. $\lambda_{\min}(\cdot)$ and $\lambda_{\max}(\cdot)$ denote the minimum and maximum eigenvalues of a matrix, respectively.

B. Graph Theory

Consider a system of N followers and one leader. The communication topology of followers is depicted by a graph $\mathcal{G} = \{\mathcal{V}, \mathcal{E}\}$ with $\mathcal{V} = \mathbb{I}_{1:N}$ and $\mathcal{E} \subseteq \mathcal{V} \times \mathcal{V}$ being the sets of vertices and edges, respectively. Define a neighbor set of node i as $\mathcal{N}_i \triangleq \{j \in \mathcal{V} | (i, j) \in \mathcal{E}\}$, where (i, j) stands for an information flow from node i to node j. The graph $\mathcal{G}$ is undirected if $(j, i) \in \mathcal{E}$ for any $(i, j) \in \mathcal{E}$. The undirected graph $\mathcal{G}$ is connected if there is a path between any node pair. The adjacency matrix of graph $\mathcal{G}$ is defined as $\boldsymbol{\mathcal{A}} = [a_{ij}] \in \mathbb{R}^{N\times N}$ with $a_{ii} = 0$, $a_{ij} = 1$ if $(i, j) \in \mathcal{E}$, and $a_{ij} = 0$, otherwise. Define a topology among followers and the leader as $\bar{\mathcal{G}} = \{\bar{\mathcal{V}}, \bar{\mathcal{E}}\}$ with $\bar{\mathcal{V}} = \mathcal{V} \cup \{0\}$ and $\bar{\mathcal{E}} \subseteq \bar{\mathcal{V}} \times \bar{\mathcal{V}}$, where the information flow from the leader to the follower is unidirectional. For the graph $\bar{\mathcal{G}}$, the corresponding degree matrix $\boldsymbol{\mathcal{D}} \in \mathbb{R}^{(N+1)\times(N+1)}$ and Laplacian matrix $\boldsymbol{\mathcal{L}} \in \mathbb{R}^{(N+1)\times(N+1)}$ can be partitioned below

$$\boldsymbol{\mathcal{D}} = \begin{bmatrix} 0 & \mathbf{0}_N^\top \\ \mathbf{0}_N & \boldsymbol{\mathcal{D}}_1 \end{bmatrix} \quad \text{and} \quad \boldsymbol{\mathcal{L}} = \begin{bmatrix} 0 & \mathbf{0}_N^\top \\ \boldsymbol{\mathcal{L}}_0 & \boldsymbol{\mathcal{L}}_1 \end{bmatrix}$$

where $\boldsymbol{\mathcal{D}}_1 = \mathrm{diag}(d_1, ..., d_N) \in \mathbb{R}^{N\times N}$, $\boldsymbol{\mathcal{L}}_1 = \boldsymbol{\mathcal{D}}_1 - \boldsymbol{\mathcal{A}} = [l_{ij}] \in \mathbb{R}^{N\times N}$, and $\boldsymbol{\mathcal{L}}_0 = \mathrm{col}(-a_{i0}) \in \mathbb{R}^N$ with $d_i = \sum_{j\in\mathcal{N}_i} a_{ij} + a_{i0}$, $l_{ii} = d_i$, and $l_{ij} = -a_{ij}$ for $i \neq j$. Here, $a_{i0} = 1$ if the follower i can access the leader, and $a_{i0} = 0$ otherwise.

C. Problem Formulation

Consider a swarm of MASs with the follower's dynamics described by

$$\dot{\boldsymbol{x}}_i(t) = \boldsymbol{A}\boldsymbol{x}_i(t) + \boldsymbol{B}\boldsymbol{u}_i(t), \quad i \in \mathbb{I}_{1:N}, \tag{1}$$

and the leader's dynamics given by

$$\dot{\boldsymbol{x}}_0(t) = \boldsymbol{A}\boldsymbol{x}_0(t) + \boldsymbol{B}\boldsymbol{u}_0(t) \tag{2}$$

where $\boldsymbol{x}_0(t) \in \mathbb{R}^n$ and $\boldsymbol{x}_i(t) \in \mathbb{R}^n$ are states of agents. $\boldsymbol{u}_0(t) \in \mathbb{R}^m$ and $\boldsymbol{u}_i(t) \in \mathbb{R}^m$ are inputs of agents. $\boldsymbol{A} \in \mathbb{R}^{n\times n}$ and $\boldsymbol{B} \in \mathbb{R}^{n\times m}$ are the system matrices to be assumed that the pair $(\boldsymbol{A}, \boldsymbol{B})$ is stabilizable. For brevity, the time variable t is omitted in the upcoming development.

To begin with, a local error $\boldsymbol{z}_i \in \mathbb{R}^n$ of agent i with respect to its neighbors is defined as follows

$$\boldsymbol{z}_i = \sum_{j\in\mathcal{N}_i} a_{ij}(\boldsymbol{x}_i - \boldsymbol{x}_j) + a_{i0}(\boldsymbol{x}_i - \boldsymbol{x}_0). \tag{3}$$

From (1)-(3), the dynamics of $\boldsymbol{z}_i$ is yielded as

$$\dot{\boldsymbol{z}}_i = \boldsymbol{A}\boldsymbol{z}_i + d_i\boldsymbol{B}\boldsymbol{u}_i - \sum_{j\in\mathcal{N}_i\cup\{0\}} a_{ij}\boldsymbol{B}\boldsymbol{u}_j. \tag{4}$$

In the consensus problem, each agent aims to synchronize with its neighbors and minimize the performance index defined by the following infinite horizon scalar function

$$J_i(\boldsymbol{z}_i, \boldsymbol{u}_i) = \int_0^\infty \Big(\boldsymbol{z}_i^\top\boldsymbol{Q}_i\boldsymbol{z}_i + \boldsymbol{u}_i^\top\boldsymbol{R}_i\boldsymbol{u}_i\Big)dt \tag{5}$$

where $\boldsymbol{Q}_i = \boldsymbol{Q}_i^\top \in \mathbb{R}^{n\times n}$ and $\boldsymbol{R}_i = \boldsymbol{R}_i^\top \in \mathbb{R}^{m\times m}$ are positive definite matrices.

Remark 1: It is observed from (4) that $J_i(\boldsymbol{z}_i, \boldsymbol{u}_i)$ depends not only on the behavior of agent i but also on that of its neighbors j for $j \in \mathcal{N}_i$. Then, function $J_i(\boldsymbol{z}_i, \boldsymbol{u}_i)$ for agent i can be explicitly rewritten as $J_i(\boldsymbol{z}_i, \boldsymbol{u}_i, \boldsymbol{u}_{-i})$ with respect to neighbor policies with $\boldsymbol{u}_{-i} = \{\boldsymbol{u}_1, \dots, \boldsymbol{u}_{i-1}, \boldsymbol{u}_{i+1}, \dots, \boldsymbol{u}_N\}$. Thus, (5) can be regarded as a differential graphical game involving multiple players $\boldsymbol{u}_{-i}$. Herein, each player optimizes its control policy against the neighbors' policies to minimize its performance index (5). The objective of this paper is to derive the optimal control policy to achieve the consensus under the differential graphical game framework.

Definition 1 ([44]): The N-tuple control policy $\{\boldsymbol{u}_i^*, \boldsymbol{u}_{-i}^*\}$ is called a Nash equilibrium solution if the inequality

$$J_i(\boldsymbol{z}_i, \boldsymbol{u}_i^*, \boldsymbol{u}_{-i}^*) \leq J_i(\boldsymbol{z}_i, \boldsymbol{u}_i, \boldsymbol{u}_{-i}^*), \quad \forall i \in \mathbb{I}_{1:N}. \tag{6}$$

holds for all players of the differential graphical game.

To seek the Nash equilibrium of the graphical game, each agent needs to update its policy $\boldsymbol{u}_i$ using the local information from communication channels. To save limited communication sources, agent i only broadcasts the latest state $\boldsymbol{x}_{is} = \boldsymbol{x}_i(t_{is})$ to its neighbors and updates its policy $\boldsymbol{u}_{is} = \boldsymbol{u}_i(t_{is})$ for $t \in [t_{is}, t_{i(s+1)})$, where $\{t_{is}\}_{s=0}^\infty$, $s \in \mathbb{N}_{>0}$ with $t_{i0} = 0$ is a sequence of triggering instants for agent i, $i \in \mathbb{I}_{1:N}$. Then, the local error dynamics of agent i with the event-based policy $\boldsymbol{u}_{is}$ can be expressed as follows

$$\dot{\boldsymbol{z}}_i = \boldsymbol{A}\boldsymbol{z}_i + d_i\boldsymbol{B}\boldsymbol{u}_{is} - \sum_{j\in\mathcal{N}_i} a_{ij}\boldsymbol{B}\boldsymbol{u}_{js} - -a_{i0}\boldsymbol{B}\boldsymbol{u}_0. \tag{7}$$

Before developing the ETM, define a error between the actual input $\boldsymbol{u}_i$ and the sampled input $\boldsymbol{u}_{is}$ as follows

$$\boldsymbol{e}_{is} = \boldsymbol{u}_{is} - \boldsymbol{u}_i. \tag{8}$$

Substituting (8) into (7), the local error dynamics of agent i is rewritten as

$$\begin{aligned}\dot{\boldsymbol{z}}_i =& \boldsymbol{A}\boldsymbol{z}_i + d_i\boldsymbol{B}(\boldsymbol{u}_i + \boldsymbol{e}_{is}) - \sum_{j\in\mathcal{N}_i} a_{ij}\boldsymbol{B}(\boldsymbol{u}_j + \boldsymbol{e}_{js}) \\ &- a_{i0}\boldsymbol{B}\boldsymbol{u}_0.\end{aligned} \tag{9}$$

To save communication resources, the larger sampling error $\boldsymbol{e}_{is}$ may result in a certain degree of control performance degradation, indicating that the sampling error plays a role against the control input. Thus, the control input and sampling error can be regarded as two players in a zero-sum game. Considering the impact of the sampling error e_{is}, we reformulate the performance index function $J_i(\boldsymbol{z}_i, \boldsymbol{u}_i)$ for agent i as

$$\begin{aligned}&J_i(\boldsymbol{z}_i, \boldsymbol{u}_i, \boldsymbol{e}_{is}) \\ &= \int_0^\infty \Big(\boldsymbol{z}_i^\top\boldsymbol{Q}_i\boldsymbol{z}_i + \boldsymbol{u}_i^\top\boldsymbol{R}_i\boldsymbol{u}_i - \mu_i^2\boldsymbol{e}_{is}^\top\boldsymbol{e}_{is}\Big)dt\end{aligned} \tag{10}$$

where $\mu_i \in \mathbb{R}_{>0}$ is a constant.

Definition 2 ([44]): The policy pair $(\boldsymbol{u}_i^*, \boldsymbol{e}_{is}^*)$ is called a Nash equilibrium of the zero-sum game if the inequality

$$J_i(\boldsymbol{z}_i, \boldsymbol{u}_i^*, \boldsymbol{e}_{is}) \leq J_i(\boldsymbol{z}_i, \boldsymbol{u}_i^*, \boldsymbol{e}_{is}^*) \leq J_i(\boldsymbol{z}_i, \boldsymbol{u}_i, \boldsymbol{e}_{is}^*) \tag{11}$$

holds for any players $\boldsymbol{u}_i$ and $\boldsymbol{e}_{is}$, $i \in \mathbb{I}_{1:N}$.

Definition 3 ([44]): The N-tuple policy pair $\{(\boldsymbol{u}_i^*, \boldsymbol{e}_{is}^*)\}_{i=1}^N$ is called the global Nash equilibrium if the inequality

$$\begin{aligned}&J_i(\boldsymbol{z}_i, \boldsymbol{u}_i^*, \boldsymbol{e}_{is}, \boldsymbol{u}_{-i}^*, \boldsymbol{e}_{-is}^*) \leq J_i(\boldsymbol{z}_i, \boldsymbol{u}_i^*, \boldsymbol{e}_{is}^*, \boldsymbol{u}_{-i}^*, \boldsymbol{e}_{-is}^*) \\ &\leq J_i(\boldsymbol{z}_i, \boldsymbol{u}_i, \boldsymbol{e}_{is}^*, \boldsymbol{u}_{-i}^*, \boldsymbol{e}_{-is}^*)\end{aligned} \tag{12}$$

holds for each agent i, $i \in \mathbb{I}_{1:N}$.

The objective of this paper is to develop an optimal event-triggered control method for the leader-follower consensus of MASs such that: 1) the optimal consensus is achieved using the formulation of differential graphical game and zero-sum game; and 2) the positive minimum interevent interval under the interval-maximum triggering mechanism is guaranteed to exclude the Zeno behavior.

To move on, the following standard assumption and necessary lemmas are provided.

Assumption 1 ([45]): The graph $\mathcal{G}$ is undirected and connected, and at least one follower has access to the leader.

Lemma 1 ([45]): Under Assumption 1, $\mathcal{L}_1$ is symmetric and positive definite, which yields the following properties:

- All eigenvalues of $\mathcal{L}_1$ hold

$$0 < \lambda_1(\mathcal{L}_1) \le \lambda_2(\mathcal{L}_1) \le \ldots \le \lambda_N(\mathcal{L}_1) = \lambda_{\max}(\mathcal{L}_1).$$

- There exists an orthogonal matrix $\boldsymbol{T}_{\mathcal{L}_1}$ such that

$$\boldsymbol{T}_{\mathcal{L}_1}^\top \mathcal{L}_1 \boldsymbol{T}_{\mathcal{L}_1} = \boldsymbol{\Lambda} = \text{diag}\{\lambda_1(\mathcal{L}_1), \lambda_2(\mathcal{L}_1), \ldots, \lambda_N(\mathcal{L}_1)\}.$$

Lemma 2 ([46]): For positive definite matrices $\boldsymbol{Q} = \boldsymbol{Q}^\top \in \mathbb{R}^{n\times n}$ and $\boldsymbol{R} = \boldsymbol{R}^\top \in \mathbb{R}^{m\times m}$ and a positive constant μ, if the pair $(\boldsymbol{A}, \boldsymbol{B})$ is stabilizable and $\boldsymbol{R}^{-1} - \boldsymbol{I}_m/\mu^2 > 0$ holds, then the symmetric positive definite matrix $\boldsymbol{P}_i = \boldsymbol{P}_i^\top \in \mathbb{R}^{n\times n}$ is the unique solution of the following game algebraic Riccati equation (GARE)

$$\boldsymbol{A}^\top \boldsymbol{P} + \boldsymbol{P}\boldsymbol{A} + \boldsymbol{Q} - \boldsymbol{P}\boldsymbol{B}(\boldsymbol{R}^{-1} - \frac{\boldsymbol{I}_m}{\mu^2})\boldsymbol{B}^\top \boldsymbol{P} = 0. \quad (13)$$

III. Main Results

This section presents the optimal event-triggered consensus method including the optimal control law and the optimal event-triggered mechanism.

A. Optimal Event-Triggered Consensus Scheme Design

To begin with, a value function for the performance index $J_i(\boldsymbol{z}_i, \boldsymbol{u}_i, \boldsymbol{e}_{is})$ is given by

$$V_i(\boldsymbol{z}_i) = \int_t^\infty \Big(\boldsymbol{z}_i^\top \boldsymbol{Q}_i \boldsymbol{z}_i + \boldsymbol{u}_i^\top \boldsymbol{R}_i \boldsymbol{u}_i - \mu_i^2 \boldsymbol{e}_{is}^\top \boldsymbol{e}_{is}\Big) d\tau \quad (14)$$

for $i \in \mathbb{I}_{1:N}$. Then, the optimal value function $V_i^*(\boldsymbol{z}_i)$ for the zero-sum game of $\boldsymbol{u}_i$ and $\boldsymbol{e}_{is}$ is defined as

$$\begin{aligned} &V_i^*(\boldsymbol{z}_i) \\ &= \min_{\boldsymbol{u}_i} \max_{\boldsymbol{e}_{is}} \int_t^\infty (\boldsymbol{z}_i^\top \boldsymbol{Q}_i \boldsymbol{z}_i + \boldsymbol{u}_i^\top \boldsymbol{R}_i \boldsymbol{u}_i - \mu_i^2 \boldsymbol{e}_{is}^\top \boldsymbol{e}_{is}) d\tau. \end{aligned} \quad (15)$$

In view of the control policy $\boldsymbol{u}_j$ and sampling error $\boldsymbol{e}_j$ of neighbor agent j for $j \in \mathcal{N}_i$, the Hamiltonian function for agent i from (9) and (14) is defined as

$$\begin{aligned} &H_i(\boldsymbol{z}_i, \boldsymbol{u}_i, \boldsymbol{e}_{is}, \nabla V_i(\boldsymbol{z}_i)) \\ &= \boldsymbol{z}_i^\top \boldsymbol{Q}_i \boldsymbol{z}_i + \boldsymbol{u}_i^\top \boldsymbol{R}_i \boldsymbol{u}_i - \mu_i^2 \boldsymbol{e}_{is}^\top \boldsymbol{e}_{is} \\ &\quad + \nabla V_i^\top(\boldsymbol{z}_i)\big(\boldsymbol{A}\boldsymbol{z}_i + d_i \boldsymbol{B}(\boldsymbol{u}_i + \boldsymbol{e}_{is}) \\ &\quad - \sum_{j\in\mathcal{N}_i} a_{ij}\boldsymbol{B}(\boldsymbol{u}_j^* + \boldsymbol{e}_{js}^*) - a_{i0}\boldsymbol{B}\boldsymbol{u}_0\big) \end{aligned} \quad (16)$$

for $i \in \mathbb{I}_{1:N}$ with $\nabla V_i(\boldsymbol{z}_i) = \partial V_i(\boldsymbol{z}_i)/\partial \boldsymbol{z}_i \in \mathbb{R}^n$.

Based on the minmax strategy, the Hamilton-Jacobi-Isaacs (HJI) equation associated with $V_i^*(\boldsymbol{z}_i)$ is formulated as [47]

$$\min_{\boldsymbol{u}_i} \max_{\boldsymbol{e}_{is}} H_i(\boldsymbol{z}_i, \boldsymbol{u}_i, \boldsymbol{e}_{is}, \nabla V_i^*(\boldsymbol{z}_i)) = 0. \quad (17)$$

Subsequently, the optimal control policy $\boldsymbol{u}_i^*$ and the optimal sampling error $\boldsymbol{e}_{is}^*$ are derived by solving $\partial H_i/\partial \boldsymbol{u}_i = 0$ and $\partial H_i/\partial \boldsymbol{e}_{is} = 0$ and presented as follows

$$\boldsymbol{u}_i^* = -\frac{d_i}{2}\boldsymbol{R}_i^{-1}\boldsymbol{B}^\top \nabla V_i^*(\boldsymbol{z}_i), \quad (18)$$

$$\boldsymbol{e}_{is}^* = \frac{d_i}{2\mu_i^2}\boldsymbol{B}^\top \nabla V_i^*(\boldsymbol{z}_i). \quad (19)$$

Substituting (18) and (19) into the HJI equation (17), it follows that

$$\begin{aligned} 0 =& \boldsymbol{z}_i^\top \boldsymbol{Q}_i \boldsymbol{z}_i - \frac{d_i^2}{4}\nabla V_i^{*\top}(\boldsymbol{z}_i)\boldsymbol{B}\boldsymbol{R}_i^{-1}\boldsymbol{B}^\top \nabla V_i^*(\boldsymbol{z}_i) \\ &+ \frac{d_i^2}{4\mu_i^2}\nabla V_i^{*\top}(\boldsymbol{z}_i)\boldsymbol{B}\boldsymbol{B}^\top \nabla V_i^*(\boldsymbol{z}_i) + \nabla V_i^{*\top}(\boldsymbol{z}_i)\boldsymbol{A}\boldsymbol{z}_i \\ &- \sum_{j\in\mathcal{N}_i} a_{ij}\nabla V_i^{*\top}(\boldsymbol{z}_i)\boldsymbol{B}(u_j^* + e_{js}^*) \\ &- a_{i0}\nabla V_i^{*\top}(\boldsymbol{z}_i)\boldsymbol{B}\boldsymbol{u}_0. \end{aligned} \quad (20)$$

The optimal sampling error $\boldsymbol{e}_{is}^*$ (19) provides the worst case input error, which can be employed to achieve the optimal consensus of MASs with the maximum sampling interval. Then, a triggering function $\hbar(e_{is}, \nabla V_i^*(\boldsymbol{z}_i))$ associated with $\boldsymbol{e}_{is}^*$ is defined as follows

$$\begin{aligned} &\hbar(e_{is}, \nabla V_i^*(\boldsymbol{z}_i)) \\ &= \boldsymbol{e}_{is}^\top \boldsymbol{e}_{is} - \frac{d_i^2}{4\mu_i^4}\nabla V_i^{*\top}(\boldsymbol{z}_i)\boldsymbol{B}\boldsymbol{B}^\top \nabla V_i^*(\boldsymbol{z}_i), \end{aligned} \quad (21)$$

which is used to develop the following optimal ETM to determine the next triggering instant

$$t_{i(s+1)} = \inf\{t > t_{is} \mid \hbar(e_{is}, \nabla V_i^*(\boldsymbol{z}_i)) \ge 0\}. \quad (22)$$

Then, it derives from (18) that the optimal event-triggered control input is

$$\boldsymbol{u}_i^*(\boldsymbol{z}_{is}) = -\frac{d_i}{2}\boldsymbol{R}_i^{-1}\boldsymbol{B}^\top \nabla V_i^*(\boldsymbol{z}_{is}), \quad (23)$$

where $\boldsymbol{z}_{is} = \boldsymbol{z}_i(t_{is}) \in \mathbb{R}^n$ is the sampled value of $\boldsymbol{z}_i(t)$ at the triggering instant t_{is}.

Remark 2: Traditional ETC schemes, such as static ETMs [48]–[51], dynamic ETMs [52]–[54], and adaptive ETMs [55], [56], are designed under the premise of system stability, where the sampling interval is expected to be as large as possible in order to reduce communication frequency and controller update. However, these approaches neglect the optimality of the triggering condition. To achieve the maximum interval sampling, this paper introduces a sampling error into the performance index and simultaneously optimizes it with the control input in a zero-sum game framework. Both the optimal control policy and triggering threshold are derived to achieve the desired system performance under the maximal sampling interval. The codesign scheme establishes a bridge between the sampling and cost to seek an equilibrium solution.

To seek the Nash equilibrium solution, assume that the optimal value function $V_i^*(\boldsymbol{z}_i)$ has the following form

$$V_i^*(\boldsymbol{z}_i) = \alpha_i \boldsymbol{z}_i^\top \boldsymbol{P}_i \boldsymbol{z}_i, \quad i \in \mathbb{I}_{1:N} \quad (24)$$

This article has been accepted for publication in IEEE Transactions on Automation Science and Engineering. This is the author's version which has not been fully edited and content may change prior to final publication. Citation information: DOI 10.1109/TASE.2026.3656938

where $\alpha_i \in \mathbb{R}_{>0}$ is a scalar gain; $\boldsymbol{P}_i = \boldsymbol{P}_i^\top > 0$ is the solution of the GARE given by Lemma 2.

Using the function $V_i^*(\boldsymbol{z}_i)$, the optimal policies from (18) and (19) are obtained below

$$\boldsymbol{u}_i^* = -\alpha_i d_i \boldsymbol{R}_i^{-1}\boldsymbol{B}^\top \boldsymbol{P}_i \boldsymbol{z}_i, \tag{25}$$

$$\boldsymbol{e}_{is}^* = \frac{\alpha_i d_i}{\mu_i^2}\boldsymbol{B}^\top \boldsymbol{P}_i \boldsymbol{z}_i. \tag{26}$$

During the interevent time, the event-based optimal policies of agent i are given by $\boldsymbol{u}_{is}^* = \boldsymbol{u}_i^*(\boldsymbol{z}_{is})$ and $\boldsymbol{e}_{is}^* = \boldsymbol{e}_{is}^*(\boldsymbol{z}_{is})$ for $t \in [t_{is}, t_{i(s+1)})$. Within the differential graphical game framework, agent i receives the control policy of neighboring agents as $\boldsymbol{u}_{js}^* = \boldsymbol{u}_j^*(\boldsymbol{z}_{js})$ and $\boldsymbol{e}_{js}^* = \boldsymbol{e}_{js}^*(\boldsymbol{z}_{js})$. Then, substitute them into the resulting closed-loop system (9) and rewrite the following form

$$\begin{aligned}\dot{\boldsymbol{z}}_i =& \boldsymbol{A}\boldsymbol{z}_i - \sum_{j=0}^{N} a_{ij}\alpha_i d_i \boldsymbol{B}(\boldsymbol{R}_i^{-1} - \frac{\boldsymbol{I}_m}{\mu_i^2})\boldsymbol{B}^\top \boldsymbol{P}_i(\boldsymbol{z}_i + \boldsymbol{e}_{iz}) \\ &+ \sum_{j\in\mathcal{N}_i} a_{ij}\alpha_j d_j \boldsymbol{B}(\boldsymbol{R}_j^{-1} - \frac{\boldsymbol{I}_m}{\mu_j^2})\boldsymbol{B}^\top \boldsymbol{P}_j(\boldsymbol{z}_j + \boldsymbol{e}_{jz}) \\ &- a_{i0}\boldsymbol{B}\boldsymbol{u}_0\end{aligned} \tag{27}$$

with $\boldsymbol{e}_{iz}(t) = \boldsymbol{z}_{is} - \boldsymbol{z}_i$ for $t \in [t_{is}, t_{i(s+1)})$, $i \in \mathbb{I}_{1:N}$.

B. Stability Analysis

To proceed the subsequent analysis, a standard assumption for the boundedness for the gradient $\nabla V_i^*(\boldsymbol{z}_i)$ is made.

Assumption 2 ([57]): For any $\epsilon_i > 0$, there exists $\delta_i > 0$ such that

$$\|\nabla V_i^*(\boldsymbol{z}_i)\| \le \epsilon_i \|\boldsymbol{z}_i\|, \quad \forall \|\boldsymbol{z}_i\| \le \delta_i. \tag{28}$$

The following theorem states that the policy pair $(\boldsymbol{u}_i^*, \boldsymbol{e}_{is}^*)$ is the Nash equilibrium defined in Definition 3.

Theorem 1: Under Assumption 2, the event-based system (9) with the optimal ETM (22) is asymptotically stable, and the policy pair $\{(\boldsymbol{u}_i^*, \boldsymbol{e}_{is}^*)\}_{i=1}^N$ constitutes the global Nash equilibrium.

Proof: Choose $V_i^*(\boldsymbol{z}_i)$ as the Lyapunov function candidate. Then, it gets from (20) that $\dot{V}_i^*(\boldsymbol{z}_i)$ holds

$$\begin{aligned}\dot{V}_i^*(\boldsymbol{z}_i) =& \nabla V_i^{*\top}\Big(\boldsymbol{A}\boldsymbol{z}_i + d_i\boldsymbol{B}\boldsymbol{u}_i^* + d_i\boldsymbol{B}\boldsymbol{e}_{is}^* \\ &- \sum_{j\in\mathcal{N}_i} a_{ij}\boldsymbol{B}(\boldsymbol{u}_j^* + \boldsymbol{e}_j^*) - a_{i0}\boldsymbol{B}\boldsymbol{u}_0\Big) \\ =& -\boldsymbol{z}_i^\top \boldsymbol{Q}_i \boldsymbol{z}_i - \frac{d_i^2}{4}\nabla V_i^{*\top}(\boldsymbol{z}_i)\boldsymbol{B}\boldsymbol{R}_i^{-1}\boldsymbol{B}^\top \nabla V_i^*(\boldsymbol{z}_i) \\ &+ \frac{d_i^2}{4\mu_i^2}\nabla V_i^{*\top}(\boldsymbol{z}_i)\boldsymbol{B}\boldsymbol{B}^\top \nabla V_i^*(\boldsymbol{z}_i).\end{aligned} \tag{29}$$

If the selection of $\boldsymbol{R}_i$ and μ_i satisfies $\boldsymbol{R}_i^{-1} - \boldsymbol{I}_m/\mu_i^2 > 0$, then it yields under Assumption 2 that

$$\begin{aligned}\dot{V}_i^*(\boldsymbol{z}_i) \le& -\lambda_{\min}(\boldsymbol{Q}_i)\|\boldsymbol{z}_i\|^2 \\ &- \frac{d_i^2}{4}\lambda_{\min}(\boldsymbol{R}_i^{-1} - \frac{\boldsymbol{I}_m}{\mu_i^2})\nabla V_i^{*\top}(\boldsymbol{z}_i)\boldsymbol{B}\boldsymbol{B}^\top \nabla V_i^*(\boldsymbol{z}_i) \\ \le& -\lambda_{\min}(\boldsymbol{Q}_i)\|\boldsymbol{z}_i\|^2 \\ &- \frac{d_i^2\epsilon_i^2}{4}\lambda_{\min}(\boldsymbol{R}_i^{-1} - \frac{\boldsymbol{I}_m}{\mu_i^2})\|\boldsymbol{B}\boldsymbol{B}^\top\|\|\boldsymbol{z}_i\|^2 \\ \le& -\ell_i\|\boldsymbol{z}_i\|^2\end{aligned} \tag{30}$$

with $\ell_i = \lambda_{\min}(\boldsymbol{Q}_i) + d_i^2\epsilon_i^2\|\boldsymbol{B}\boldsymbol{B}\|\lambda_{\min}(\boldsymbol{R}_i^{-1} - \boldsymbol{I}_m/\mu_i^2)/4 > 0$, which yields that $\dot{V}_i^*(\boldsymbol{z}_i) \le 0$. Consequently, it is concluded that the event-based system in (9) is stable, and that all agents using the optimal control input and the optimal ETM (22) can reach the consensus.

Remark 3: In this paper, $\boldsymbol{Q}_i$, $\boldsymbol{R}_i$, μ_i, and α_i are critical parameters that determine the system performance and resource conservation. To guide practical implementation, a tuning strategy is provided as follows. Specifically, the selection of $\boldsymbol{Q}_i$, $\boldsymbol{R}_i$, and μ_i should guarantee that the function $V_i^*(\boldsymbol{z}_i)$ is negative definite. The larger $\boldsymbol{Q}_i$ can accelerate the convergence of consensus error but may require more control efforts. The larger $\boldsymbol{R}_i$ results in lower control at the cost of slower convergence. According to (14), (19), (22), and (30), a smaller μ_i allows a larger interevent interval to reduce the triggering number but degrade the consensus performance, that implies the stronger robustness against event-based error. The larger α_i raises both the magnitude of control input and triggering threshold, which accelerate convergence of the value function. Therefore, $\boldsymbol{Q}_i$, $\boldsymbol{R}_i$, μ_i, and α_i should be chosen to adjust the tradeoff between the expected performance and sampling frequency.

In what follows, we will illustrate that the policy pair $(\boldsymbol{u}_i^*, \boldsymbol{e}_{is}^*)$ constitutes the Nash equilibrium of the game. Given that $V_i^*(\boldsymbol{z}_i(\infty)) = V_i^*(0) = 0$, the function $J_i(\boldsymbol{z}_i, \boldsymbol{u}_i, \boldsymbol{e}_{is})$ in (10) is reformulated as

$$\begin{aligned}&J_i(\boldsymbol{z}_i, \boldsymbol{u}_i, \boldsymbol{e}_{is}) \\ &= \int_0^\infty (\boldsymbol{z}_i^\top \boldsymbol{Q}_i \boldsymbol{z}_i + \boldsymbol{u}_i^\top \boldsymbol{R}_i \boldsymbol{u}_i - \mu_i^2 \boldsymbol{e}_{is}^\top \boldsymbol{e}_{is})dt \\ &\quad + V_i^*(\boldsymbol{z}_i(0)) + \int_0^\infty \nabla V_i^{*\top}(\boldsymbol{z}_i)\Big(\boldsymbol{A}\boldsymbol{z}_i + d_i\boldsymbol{B}\boldsymbol{u}_i \\ &\quad + d_i\boldsymbol{B}\boldsymbol{e}_{is} - \sum_{j\in\mathcal{N}_i} a_{ij}\boldsymbol{B}(\boldsymbol{u}_j + \boldsymbol{e}_{js}) - a_{i0}\boldsymbol{B}\boldsymbol{u}_0\Big)dt.\end{aligned} \tag{31}$$

According to the fact that $d_i\nabla V_i^{*\top}\boldsymbol{B}\boldsymbol{u}_i = -2\boldsymbol{u}_i^{*\top}\boldsymbol{R}_i\boldsymbol{u}_i$ and $d_i\nabla V_i^{*\top}\boldsymbol{B}\boldsymbol{e}_{is} = 2\mu_i^2\boldsymbol{e}_{is}^{*\top}\boldsymbol{e}_{is}$ from (18) and (19), it implies that

$$\begin{aligned}&J_i(\boldsymbol{z}_i, \boldsymbol{u}_i, \boldsymbol{e}_{is}) \\ &= \int_0^\infty (\boldsymbol{z}_i^\top \boldsymbol{Q}_i \boldsymbol{z}_i + (\boldsymbol{u}_i - \boldsymbol{u}_i^*)^\top \boldsymbol{R}_i \boldsymbol{u}_i - \boldsymbol{u}_i^\top \boldsymbol{R}_i \boldsymbol{u}_i^* \\ &- \mu_i^2(\boldsymbol{e}_{is} - \boldsymbol{e}_{is}^*)^\top \boldsymbol{e}_{is} + \mu_i^2 \boldsymbol{e}_{is}^\top \boldsymbol{e}_{is}^*)dt + V_i^*(\boldsymbol{z}_i(0)) \\ &+ \int_0^\infty \nabla V_i^{*\top}(\boldsymbol{A}\boldsymbol{z}_i - \sum_{j\in\mathcal{N}_i} a_{ij}\boldsymbol{B}(\boldsymbol{u}_j + \boldsymbol{e}_j) - a_{i0}\boldsymbol{B}\boldsymbol{u}_0)dt.\end{aligned}$$

Since $(\boldsymbol{u}_i - \boldsymbol{u}_i^*)^\top \boldsymbol{R}_i \boldsymbol{u}_i - \boldsymbol{u}_i^\top \boldsymbol{R}_i \boldsymbol{u}_i^* = (\boldsymbol{u}_i - \boldsymbol{u}_i^*)^\top \boldsymbol{R}_i(\boldsymbol{u}_i - \boldsymbol{u}_i^*) - \boldsymbol{u}_i^{*\top}\boldsymbol{R}_i\boldsymbol{u}_i^*$ and $-\mu_i^2(\boldsymbol{e}_{is} - \boldsymbol{e}_{is}^*)^\top \boldsymbol{e}_{is} + \mu_i^2 \boldsymbol{e}_{is}^{*\top}\boldsymbol{e}_{is} = -\mu_i^2(\boldsymbol{e}_{is} - \boldsymbol{e}_{is}^*)^\top(\boldsymbol{e}_{is} - \boldsymbol{e}_{is}^*) + \mu_i^2\boldsymbol{e}_{is}^{*\top}\boldsymbol{e}_{is}^*$, we rewrite $J_i(\boldsymbol{z}_i, \boldsymbol{u}_i, \boldsymbol{e}_{is})$ as

$$\begin{aligned}J_i(\boldsymbol{z}_i, \boldsymbol{u}_i, \boldsymbol{e}_{is}) =& V_i^*(\boldsymbol{z}_i(0)) + \int_0^\infty \Big(\boldsymbol{z}_i^\top \boldsymbol{Q}_i \boldsymbol{z}_i + \boldsymbol{u}_i^{*\top}\boldsymbol{R}_i\boldsymbol{u}_i^* \\ &- \mu_i^2\boldsymbol{e}_{is}^{*\top}\boldsymbol{e}_{is}^* + \nabla V_i^{*\top}\big(\boldsymbol{A}\boldsymbol{z}_i + d_i\boldsymbol{B}\boldsymbol{u}_i^* + d_i\boldsymbol{B}\boldsymbol{e}_{is}^* - a_{i0}\boldsymbol{B}\boldsymbol{u}_0\end{aligned}$$

$$- \sum_{j\in\mathcal{N}_i} a_{ij}\boldsymbol{B}(\boldsymbol{u}_j+\boldsymbol{e}_j))\Big)dt + \int_0^\infty \big((\boldsymbol{u}_i-\boldsymbol{u}_i^*)^\top \boldsymbol{R}_i(\boldsymbol{u}_i-\boldsymbol{u}_i^*) - \mu_i^2(\boldsymbol{e}_{is}-\boldsymbol{e}_{is}^*)^\top(\boldsymbol{e}_{is}-\boldsymbol{e}_{is}^*)\big)dt.$$

Suppose that neighbor policies employ $\boldsymbol{u}_j = \boldsymbol{u}_j^*$ and $\boldsymbol{e}_{js} = \boldsymbol{e}_{js}^*$. Then, one obtains from (17) that

$$J_i(\boldsymbol{z}_i,\boldsymbol{u}_i,\boldsymbol{e}_{is}) = V_i^*(\boldsymbol{z}_i(0)) + \int_0^\infty \big((\boldsymbol{u}_i-\boldsymbol{u}_i^*)^\top \boldsymbol{R}_i(\boldsymbol{u}_i-\boldsymbol{u}_i^*) - \mu_i^2(\boldsymbol{e}_{is}-\boldsymbol{e}_{is}^*)^\top(\boldsymbol{e}_{is}-\boldsymbol{e}_{is}^*)\big)dt. \quad (32)$$

Further, (32) is given by the following cases

$$J_i(\boldsymbol{z}_i,\boldsymbol{u}_i,\boldsymbol{e}_{is}) = \begin{cases} V_i^*(\boldsymbol{z}_i(0)) + \int_0^\infty (\boldsymbol{u}_i-\boldsymbol{u}_i^*)^\top \boldsymbol{R}_i(\boldsymbol{u}_i-\boldsymbol{u}_i^*)dt, & \text{for } \boldsymbol{u}_i \neq \boldsymbol{u}_i^*, \quad \boldsymbol{e}_{is}=\boldsymbol{e}_{is}^*, \\ V_i^*(\boldsymbol{z}_i(0)), & \text{for } \boldsymbol{u}_i = \boldsymbol{u}_i^*, \quad \boldsymbol{e}_{is}=\boldsymbol{e}_{is}^*, \\ V_i^*(\boldsymbol{z}_i(0)) - \int_0^\infty \mu_i^2(\boldsymbol{e}_{is}-\boldsymbol{e}_{is}^*)^\top(\boldsymbol{e}_{is}-\boldsymbol{e}_{is}^*)dt, & \text{for } \boldsymbol{u}_i = \boldsymbol{u}_i^*, \quad \boldsymbol{e}_{is}\neq\boldsymbol{e}_{is}^*. \end{cases} \quad (33)$$

As a result, it follows from (33) that $J_i(\boldsymbol{z}_i(0),\boldsymbol{u}_i^*,\boldsymbol{e}_{is}) \le J_i(\boldsymbol{z}_i(0),\boldsymbol{u}_i^*,\boldsymbol{e}_{is}^*) \le J_i(\boldsymbol{z}_i(0),\boldsymbol{u}_i,\boldsymbol{e}_{is}^*)$. For the zero-sum game of players $\boldsymbol{u}_i$ and $\boldsymbol{e}_{is}$, the control input $\boldsymbol{u}_i^*$ is the optimal solution to minimize $J_i(\boldsymbol{z}_i,\boldsymbol{u}_i,\boldsymbol{e}_{is})$ against the maximal sampling interval $\boldsymbol{e}_{is}^*$. Moreover, the policy pair $(\boldsymbol{u}_i^*,\boldsymbol{e}_{is}^*)$ also minimizes $J_i(\boldsymbol{z}_i,\boldsymbol{u}_i,\boldsymbol{e}_{is})$ against the neighbor pair $(\boldsymbol{u}_j^*,\boldsymbol{e}_{js}^*)$ for $j\in\mathcal{N}_i$. When the condition holds for each agent i for $i\in\mathbb{I}_{1:N}$, then $\{(\boldsymbol{u}_i^*,\boldsymbol{e}_{is}^*)\}_{i=1}^N$ constitutes the global Nash equilibrium of the differential graphical game. □

Remark 4: For traditional event-triggered optimal control schemes in [58] and references therein, one has $J_i(\boldsymbol{z}_i(0),\boldsymbol{u}_i^*) \to V_i^*(\boldsymbol{z}_i(0))$ as the quantization term is close to zero by increasing the sampling frequency, which asymptotically approaches the performance of the time-triggered controller. By contrast, our game-based scheme establishes directly that the optimal value holds $J_i(\boldsymbol{z}_i(0),\boldsymbol{u}_i^*,\boldsymbol{e}_{is}^*) = V_i^*(\boldsymbol{z}_i(0))$ from (33). Therefore, it shows that our proposed method presents a superior optimization result to traditional control schemes.

To facilitate the subsequent analysis, matrices $\boldsymbol{P}_i$, $\boldsymbol{Q}_i$, and $\boldsymbol{R}_i$, as well as the parameter μ_i of all agent are set to be same, i.e., $\boldsymbol{P}_i \triangleq \boldsymbol{P}$, $\boldsymbol{Q}_i \triangleq \boldsymbol{Q}$, $\boldsymbol{R}_i \triangleq \boldsymbol{R}$, and $\mu_i \triangleq \mu$. Denote $\boldsymbol{z} = \mathrm{col}(\boldsymbol{z}_1,...,\boldsymbol{z}_N)$, $\boldsymbol{e}_z(t) = \mathrm{col}(\boldsymbol{e}_{1z}(t),...,\boldsymbol{e}_{Nz}(t))$, and $\boldsymbol{\alpha} = \mathrm{diag}(\alpha_1,...,\alpha_N)$. Then, rewrite the resulting closed-loop system (27) as the following compact form

$$\begin{aligned}\dot{\boldsymbol{z}} =& \big(\boldsymbol{I}_N\otimes\boldsymbol{A} - \boldsymbol{\mathcal{L}}_1\boldsymbol{\mathcal{D}}_1\boldsymbol{\alpha}\otimes\boldsymbol{B}(\boldsymbol{R}^{-1}-\frac{\boldsymbol{I}_m}{\mu^2})\boldsymbol{B}^\top\boldsymbol{P}\big)\boldsymbol{z} \\ &- \big(\boldsymbol{\mathcal{L}}_1\boldsymbol{\mathcal{D}}_1\boldsymbol{\alpha}\otimes\boldsymbol{B}(\boldsymbol{R}^{-1}-\frac{\boldsymbol{I}_m}{\mu^2})\boldsymbol{B}^\top\boldsymbol{P}\big)\boldsymbol{e}_z(t) \\ &+ (\boldsymbol{\mathcal{L}}_0\otimes\boldsymbol{B})\boldsymbol{u}_0. \end{aligned} \quad (34)$$

Theorem 2: Consider the MAS (1) with the optimal event-triggered control policy (23), the optimal value function (24), and the optimal event-triggered mechanism (22). Under *Assumptions* 1 and 2 and $\alpha_i \ge 1/(2\min\{d_i\}\lambda_{\min}(\boldsymbol{\mathcal{L}}_1))$, we have 1) if the input of the leader is zero, the system (34) is exponentially stable; 2) if the input of the leader is bounded, the system (34) is input-to-state stable.

Proof: Consider a Lyapunov function candidate as

$$L = \boldsymbol{z}^\top(\boldsymbol{\mathcal{L}}_1\otimes\boldsymbol{P})\boldsymbol{z} + \boldsymbol{z}_s^\top(\boldsymbol{\mathcal{L}}_1\otimes\boldsymbol{P})\boldsymbol{z}_s \quad (35)$$

with $\boldsymbol{z}_s = \mathrm{col}(\boldsymbol{z}_{1s},...,\boldsymbol{z}_{Ns})$.

Case 1: For $t\in(t_{is},t_{i(s+1)})$, $s\in\{0,1,...\}$, the event-based error $\boldsymbol{z}_{is}$ holds a constant, which implies that the derivative of $\boldsymbol{z}_s^\top(\boldsymbol{\mathcal{L}}_1\otimes\boldsymbol{P})\boldsymbol{z}_s$ is equal to zero.

Differentiating L along (34), we have

$$\begin{aligned}\dot{L} =& \boldsymbol{z}^\top\Big(\boldsymbol{\mathcal{L}}_1\otimes(\boldsymbol{A}^\top\boldsymbol{P}+\boldsymbol{P}\boldsymbol{A})\Big)\boldsymbol{z} \\ &- \boldsymbol{z}^\top\Big(\boldsymbol{\alpha}\boldsymbol{\mathcal{D}}_1\boldsymbol{\mathcal{L}}_1\otimes\boldsymbol{P}\boldsymbol{B}(\boldsymbol{R}^{-1}-\frac{\boldsymbol{I}_m}{\mu^2})\boldsymbol{B}^\top\Big)(\boldsymbol{\mathcal{L}}_1\otimes\boldsymbol{P})\boldsymbol{z} \\ &- \boldsymbol{z}^\top(\boldsymbol{\mathcal{L}}_1\otimes\boldsymbol{P})\Big(\boldsymbol{\mathcal{L}}_1\boldsymbol{\mathcal{D}}_1\boldsymbol{\alpha}\otimes\boldsymbol{B}(\boldsymbol{R}^{-1}-\frac{\boldsymbol{I}_m}{\mu^2})\boldsymbol{B}^\top\boldsymbol{P}\Big)\boldsymbol{z} \\ &- 2\boldsymbol{z}^\top\Big(\boldsymbol{\mathcal{L}}_1^2\boldsymbol{\mathcal{D}}_1\boldsymbol{\alpha}\otimes\boldsymbol{P}\boldsymbol{B}(\boldsymbol{R}^{-1}-\frac{\boldsymbol{I}_m}{\mu^2})\boldsymbol{B}^\top\boldsymbol{P}\Big)\boldsymbol{e}_z(t) \\ &- 2\boldsymbol{z}^\top(\boldsymbol{\mathcal{L}}_1\otimes\boldsymbol{P})(\boldsymbol{\mathcal{L}}_0\otimes\boldsymbol{B})\boldsymbol{u}_0. \end{aligned} \quad (36)$$

Substituting (13) into (36), $\dot{L}$ is further given by

$$\begin{aligned}\dot{L} =& -\boldsymbol{z}^\top(\boldsymbol{\mathcal{L}}_1\otimes\boldsymbol{Q})\boldsymbol{z} \\ &- \boldsymbol{z}^\top\Big((2\boldsymbol{\mathcal{L}}_1^2\boldsymbol{\mathcal{D}}_1\boldsymbol{\alpha}-\boldsymbol{\mathcal{L}}_1)\otimes\boldsymbol{P}\boldsymbol{B}(\boldsymbol{R}^{-1}-\frac{\boldsymbol{I}_m}{\mu^2})\boldsymbol{B}^\top\boldsymbol{P}\Big)\boldsymbol{z} \\ &- 2\boldsymbol{z}^\top\Big(\boldsymbol{\mathcal{L}}_1^2\boldsymbol{\mathcal{D}}_1\boldsymbol{\alpha}\otimes\boldsymbol{P}\boldsymbol{B}(\boldsymbol{R}^{-1}-\frac{\boldsymbol{I}_m}{\mu^2})\boldsymbol{B}^\top\boldsymbol{P}\Big)\boldsymbol{e}_z(t) \\ &- 2\boldsymbol{z}^\top(\boldsymbol{\mathcal{L}}_1\otimes\boldsymbol{P})(\boldsymbol{\mathcal{L}}_0\otimes\boldsymbol{B})\boldsymbol{u}_0. \end{aligned} \quad (37)$$

According to Lemma 1, it follows that $\boldsymbol{\mathcal{L}}_1 = \boldsymbol{T}_{\mathcal{L}_1}\boldsymbol{\Lambda}\boldsymbol{T}_{\mathcal{L}_1}^\top$ and $\boldsymbol{\mathcal{L}}_1^2 = \boldsymbol{T}_{\mathcal{L}_1}\boldsymbol{\Lambda}^2\boldsymbol{T}_{\mathcal{L}_1}^\top$. Utilizing $\mu^2\boldsymbol{I}_m > \boldsymbol{R}$, one has

$$\boldsymbol{z}^\top(\boldsymbol{\mathcal{L}}_1\otimes\boldsymbol{Q})\boldsymbol{z} = \boldsymbol{\zeta}^\top(\boldsymbol{\Lambda}\otimes\boldsymbol{Q})\boldsymbol{\zeta} = \sum_{i=1}^N \lambda_i\boldsymbol{\zeta}_i^\top\boldsymbol{Q}\boldsymbol{\zeta}_i, \quad (38)$$

$$\boldsymbol{z}^\top(\boldsymbol{\mathcal{L}}_1\boldsymbol{\mathcal{L}}_0\otimes\boldsymbol{P}\boldsymbol{B})\boldsymbol{u}_0 = \boldsymbol{\zeta}^\top(\boldsymbol{\Lambda}\boldsymbol{T}_{\mathcal{L}_1}^\top\boldsymbol{\mathcal{L}}_0\otimes\boldsymbol{P}\boldsymbol{B})\boldsymbol{u}_0, \quad (39)$$

$$\begin{aligned}&\boldsymbol{z}^\top\Big(\boldsymbol{\mathcal{L}}_1^2\boldsymbol{\mathcal{D}}_1\boldsymbol{\alpha}\otimes\boldsymbol{P}\boldsymbol{B}(\boldsymbol{R}^{-1}-\frac{\boldsymbol{I}_m}{\mu^2})\boldsymbol{B}^\top\boldsymbol{P}\Big)\boldsymbol{e}_z(t) \\ &= \boldsymbol{\zeta}^\top\Big(\boldsymbol{\Lambda}^2\boldsymbol{T}_{\mathcal{L}_1}^\top\boldsymbol{\mathcal{D}}_1\boldsymbol{\alpha}\otimes\boldsymbol{P}\boldsymbol{B}(\boldsymbol{R}^{-1}-\frac{\boldsymbol{I}_m}{\mu^2})\boldsymbol{B}^\top\boldsymbol{P}\Big)\boldsymbol{e}_z(t), \end{aligned} \quad (40)$$

and

$$\begin{aligned}&\boldsymbol{z}^\top\Big((2\boldsymbol{\mathcal{L}}_1^2\boldsymbol{\mathcal{D}}_1\boldsymbol{\alpha}-\boldsymbol{\mathcal{L}}_1)\otimes\boldsymbol{P}\boldsymbol{B}(\boldsymbol{R}^{-1}-\frac{\boldsymbol{I}_m}{\mu^2})\boldsymbol{B}^\top\boldsymbol{P}\Big)\boldsymbol{z} \\ &\ge \boldsymbol{z}^\top\Big((2\underline{\alpha}\underline{d}\boldsymbol{\mathcal{L}}_1^2-\boldsymbol{\mathcal{L}}_1)\otimes\boldsymbol{P}\boldsymbol{B}(\boldsymbol{R}^{-1}-\frac{\boldsymbol{I}_m}{\mu^2})\boldsymbol{B}^\top\boldsymbol{P}\Big)\boldsymbol{z} \\ &= \boldsymbol{z}^\top(\boldsymbol{T}_{\boldsymbol{\mathcal{L}}_1}\otimes\boldsymbol{I}_m)\Big((2\underline{\alpha}\underline{d}\boldsymbol{\Lambda}^2-\boldsymbol{\Lambda})\otimes\boldsymbol{P}\boldsymbol{B}(\boldsymbol{R}^{-1}-\frac{\boldsymbol{I}_m}{\mu^2}) \\ &\qquad\times\boldsymbol{B}^\top\boldsymbol{P}\Big)(\boldsymbol{T}_{\mathcal{L}_1}^\top\otimes\boldsymbol{I}_n)\boldsymbol{z} \\ &= \boldsymbol{\zeta}^\top\Big((2\underline{\alpha}\underline{d}\boldsymbol{\Lambda}^2-\boldsymbol{\Lambda})\otimes\boldsymbol{P}\boldsymbol{B}(\boldsymbol{R}^{-1}-\frac{\boldsymbol{I}_n}{\mu^2})\boldsymbol{B}^\top\boldsymbol{P}\Big)\boldsymbol{\zeta}, \end{aligned} \quad (41)$$

where $\underline{\alpha} = \min_{i\in\mathbb{I}_{1:N}}\{\alpha_i\}$, $\underline{d} = \min_{i\in\mathbb{I}_{1:N}}\{d_i\}$, and $\boldsymbol{\zeta} = \mathrm{col}\{\boldsymbol{\zeta}_1,\dots,\boldsymbol{\zeta}_N\} = (\boldsymbol{T}_{\mathcal{L}_1}^\top\otimes\boldsymbol{I}_n)\boldsymbol{z}$.

Based on the results in (38)-(41), $\dot{L}$ is presented as

$$\dot{L} \le -\sum_{i=1}^N \lambda_i\boldsymbol{\zeta}_i^\top\boldsymbol{Q}\boldsymbol{\zeta}_i$$

$$
\begin{aligned}
&- \boldsymbol{\zeta}^\top \Big((2\underline{\alpha}\underline{d}\boldsymbol{\Lambda}^2 - \boldsymbol{\Lambda}) \otimes \boldsymbol{PB}(\boldsymbol{R}^{-1} - \frac{\boldsymbol{I}_m}{\mu^2})\boldsymbol{B}^\top \boldsymbol{P} \Big)\boldsymbol{\zeta} \\
&- 2\boldsymbol{\zeta}^\top \Big(\boldsymbol{\Lambda}^2 \boldsymbol{T}_{\mathcal{L}_1}^\top \boldsymbol{\mathcal{D}_1 \alpha} \otimes \boldsymbol{PB}(\boldsymbol{R}^{-1} - \frac{\boldsymbol{I}_m}{\mu^2})\boldsymbol{B}^\top \boldsymbol{P} \Big)\boldsymbol{e}_z \\
&- 2\boldsymbol{\zeta}^\top (\boldsymbol{\Lambda} \boldsymbol{T}_{\mathcal{L}_1}^\top \boldsymbol{\mathcal{L}}_0 \otimes \boldsymbol{PB})\boldsymbol{u}_0. \qquad (42)
\end{aligned}
$$

It is clear that we choose $\underline{\alpha} \geq 1/(2\underline{d}\lambda_{\min}(\boldsymbol{\mathcal{L}}_1))$ such that $(2\underline{\alpha}\underline{d}\boldsymbol{\Lambda}^2 - \boldsymbol{\Lambda}) \otimes \boldsymbol{PB}(\boldsymbol{R}^{-1} - \boldsymbol{I}_m/\mu^2)\boldsymbol{B}^\top\boldsymbol{P}$ is positive semidefinite. Then, it follows that

$$
\begin{aligned}
\dot{L} \leq& -\sum_{i=1}^{N} \lambda_i \boldsymbol{\zeta}_i^\top \boldsymbol{Q}\boldsymbol{\zeta}_i \\
&+ \frac{1}{\gamma_1}\boldsymbol{\zeta}^\top \big(\boldsymbol{\Lambda}^2 \otimes \boldsymbol{PBB}^\top\boldsymbol{P}\big)\boldsymbol{\zeta} + \gamma_1 \boldsymbol{u}_0^\top(\boldsymbol{\mathcal{L}}_0^\top \boldsymbol{\mathcal{L}}_0 \otimes \boldsymbol{I}_m)\boldsymbol{u}_0 \\
&+ \frac{1}{\gamma_2}\boldsymbol{\zeta}^\top \big(\boldsymbol{\Lambda}^4 \otimes \boldsymbol{PBB}^\top\boldsymbol{P}\big)\boldsymbol{\zeta} + \gamma_2 \boldsymbol{e}_z^\top(\boldsymbol{\mathcal{D}}_1^2\boldsymbol{\alpha}^2 \otimes \boldsymbol{M})\boldsymbol{e}_z
\end{aligned} \qquad (43)
$$

where $\boldsymbol{M} = \boldsymbol{PB}(\boldsymbol{R}^{-1} - \boldsymbol{I}_m/\mu^2)^2\boldsymbol{B}^\top\boldsymbol{P}$, and γ_1 and γ_2 are positive constants.

According to the optimal ETM (22), it gets that $\hbar \leq 0$ for the interevent interval $t \in (t_{is}, t_{i(s+1)})$, namely,

$$
\boldsymbol{e}_{is}^\top \boldsymbol{e}_{is} \leq \boldsymbol{e}_{is}^{*\top}\boldsymbol{e}_{is}^*. \qquad (44)
$$

Furthermore, it yields from (8) and (25) that $\boldsymbol{e}_{is} = -\alpha_i d_i \boldsymbol{R}^{-1}\boldsymbol{B}^\top\boldsymbol{P}(\boldsymbol{z}_{is} - \boldsymbol{z}_i) = -\alpha_i d_i \boldsymbol{R}^{-1}\boldsymbol{B}^\top\boldsymbol{P}\boldsymbol{e}_{iz}$, which and (26) are substituted into the inequality (44). Then, we have $\boldsymbol{e}_{iz}^\top\boldsymbol{PBR}^{-2}\boldsymbol{B}^\top\boldsymbol{P}\boldsymbol{e}_{iz} \leq \boldsymbol{z}_i^\top\boldsymbol{PBB}^\top\boldsymbol{P}\boldsymbol{z}_i/\mu^4$, which further derives that $\boldsymbol{e}_{iz}^\top\boldsymbol{PBB}^\top\boldsymbol{P}\boldsymbol{e}_{iz} \leq \boldsymbol{z}_i^\top\boldsymbol{PBB}^\top\boldsymbol{P}\boldsymbol{z}_i$ using the condition $\boldsymbol{R}^{-1} > \boldsymbol{I}_m/\mu^2$. To move on, it follows that $\boldsymbol{e}_{iz}^\top\boldsymbol{e}_{iz} \leq \lambda_{\max}(\boldsymbol{PBB}^\top\boldsymbol{P})\boldsymbol{z}_i^\top\boldsymbol{z}_i/\lambda_{\min}(\boldsymbol{PBB}^\top\boldsymbol{P})$. Noting that the fact $\boldsymbol{z}^\top\boldsymbol{z} = \boldsymbol{\zeta}^\top(\boldsymbol{T}_{\mathcal{L}_1}^\top\boldsymbol{T}_{\mathcal{L}_1} \otimes \boldsymbol{I}_m)\boldsymbol{\zeta} = \boldsymbol{\zeta}^\top\boldsymbol{\zeta}$, then one has

$$
\dot{L} \leq -\theta_1\boldsymbol{\zeta}^\top\boldsymbol{\zeta} + \theta_2\boldsymbol{u}_0^\top\boldsymbol{u}_0 \qquad (45)
$$

with

$$
\begin{aligned}
\theta_1 =& \lambda_1\lambda_{\min}(\boldsymbol{Q}) - \frac{\gamma_1\lambda_1^4 + \gamma_2\lambda_1^2}{\gamma_1\gamma_2}\|\boldsymbol{PBB}^\top\boldsymbol{P}\| \\
&- \gamma_2\bar{\alpha}^2\bar{d}^2\|\boldsymbol{M}\|\frac{\lambda_{\max}(\boldsymbol{PBB}^\top\boldsymbol{P})}{\lambda_{\min}(\boldsymbol{PBB}^\top\boldsymbol{P})}, \qquad (46) \\
\theta_2 =& \gamma_1\|\boldsymbol{\mathcal{L}}_0\|^2, \qquad (47)
\end{aligned}
$$

where $\bar{\alpha} = \max_{i\in\mathbb{I}_{1:N}}\{\alpha_i\}$ and $\bar{d} = \max_{i\in\mathbb{I}_{1:N}}\{d_i\}$. Choose appreciate γ_1, γ_2, and α such that $\theta_1 > 0$. When the leader holds the zero input, i.e. $\boldsymbol{u}_0 = \boldsymbol{0}_m$, the resulting system (34) is exponentially stable, which implies from (45) that $\lim_{t\to\infty}\boldsymbol{z} = \boldsymbol{0}_{nN}$ exponentially. If the input $\boldsymbol{u}_0$ is bounded satisfying $\|\boldsymbol{u}_0\| \leq \bar{u}_0$ with $\bar{u}_0 \in \mathbb{R}_{>0}$, we have

$$
\dot{L} \leq -\theta_1(1-\xi)\boldsymbol{\zeta}^\top\boldsymbol{\zeta} < 0
$$

for $\|\boldsymbol{\zeta}\| \geq \sqrt{\theta_2/(\theta_1\xi)}\bar{u}_0$ with $0 < \xi < 1$. Then, it is concluded the system (27) is input-to-state stable.

Case 2: For the discrete instant $t = t_{i(s+1)}$, $s \in \{0, 1, ...\}$, the difference of a Lyapunov function $L_i = \boldsymbol{z}_i^\top\boldsymbol{P}\boldsymbol{z}_i + \boldsymbol{z}_{is}^\top\boldsymbol{P}\boldsymbol{z}_{is}$ for agent i is presented as

$$
\Delta L_i = L_i(t_{i(s+1)}) - L_i(t_{i(s+1)}^-) = \Delta L_{i1} + \Delta L_{i2} \qquad (48)
$$

with $\Delta L_{i1} = \boldsymbol{z}_i(t_{i(s+1)})^\top\boldsymbol{P}\boldsymbol{z}_i(t_{i(s+1)}) - \boldsymbol{z}_i(t_{i(s+1)}^-)^\top\boldsymbol{P} \times \boldsymbol{z}_i(t_{i(s+1)}^-)$ and $\Delta L_{i2} = \boldsymbol{z}_{i(s+1)}^\top\boldsymbol{P}\boldsymbol{z}_{i(s+1)} - \boldsymbol{z}_{is}^\top\boldsymbol{P}\boldsymbol{z}_{is}$. According to the triggering mechanism (22), it leads to $\Delta L_{i1} \leq 0$ and $\Delta L_{i2} \leq -\kappa(\|\Delta\boldsymbol{z}_{i(s+1)}\|)$ for $\forall t \in (t_s, t_{i(s+1)})$, where $\Delta\boldsymbol{z}_{i(s+1)} = \boldsymbol{z}_{i(s+1)} - \boldsymbol{z}_{is}$ and $\kappa(\cdot)$ is a class-$\mathcal{K}$ function. Then, it shows that the function L_i, $i \in \mathbb{I}_{1:N}$ is decreasing at the instant $t_i = t_{i(s+1)}$, $s \in \{0, 1, ...\}$.

According to the resulting conclusion, it shows that all error signals of the closed-loop system are bounded. □

To proceed, we will prove that Zeno-free behavior can be guaranteed using our proposed optimal ETM.

Theorem 3: Under the conditions given in Theorem 2, it guarantees the existence of a positive minimum sampling interval and exclusion of Zeno behavior for each agent.

Proof: Taking the derivative of $\boldsymbol{e}_{iz}(t)$, we have

$$
\dot{\boldsymbol{e}}_{iz}(t) = -\dot{\boldsymbol{z}}_i, \qquad (49)
$$

which implies from (27)

$$
\begin{aligned}
&\|\dot{\boldsymbol{e}}_{iz}(t)\| \\
&= \|\boldsymbol{A}\boldsymbol{e}_{iz}(t) - \boldsymbol{A}\boldsymbol{z}_{is} + \alpha_i d_i^2 \boldsymbol{B}(\boldsymbol{R}_i^{-1} - \frac{\boldsymbol{I}_m}{\mu_i^2})\boldsymbol{B}^\top\boldsymbol{P}_i\boldsymbol{z}_{is} \\
&\quad - \sum_{j\in\mathcal{N}_i} a_{ij}\alpha_j d_j \boldsymbol{B}(\boldsymbol{R}_j^{-1} - \frac{\boldsymbol{I}_m}{\mu_j^2})\boldsymbol{B}^\top\boldsymbol{P}_j\boldsymbol{z}_j(t_{js'}) + a_{i0}\boldsymbol{B}\boldsymbol{u}_0\| \\
&\leq \|\boldsymbol{A}\|\|\boldsymbol{e}_{iz}(t)\| + \|\boldsymbol{B}\|_{\mathrm{F}}\bar{u}_0 + \beta_i \qquad (50)
\end{aligned}
$$

for $t \in [t_{is}, t_{i(s+1)})$, $i \in \mathbb{I}_{1:N}$, where $\beta_i = \max\|\boldsymbol{A}\boldsymbol{z}_{is} - \alpha_i d_i^2\boldsymbol{B}(\boldsymbol{R}_i^{-1} - \boldsymbol{I}_m/\mu_i^2)\boldsymbol{B}^\top\boldsymbol{P}_i\boldsymbol{z}_{is} + \sum_{j\in\mathcal{N}_i} a_{ij} \times \alpha_j d_j \boldsymbol{B}(\boldsymbol{R}_j^{-1} - \boldsymbol{I}_m/\mu_j^2)\boldsymbol{B}^\top\boldsymbol{P}_j\boldsymbol{z}_j(t_{js'})\|$ and $t_{js'} = \arg\max_{s\in\{0,1,...\}}\{t_{js}|t_{js} \leq t, j \in \mathcal{N}_i\}$.

By solving the inequality (50), it obtains

$$
\|\boldsymbol{e}_{iz}(t)\| \leq \frac{\beta_i + \|\boldsymbol{B}\|_{\mathrm{F}}\bar{u}_0}{\|\boldsymbol{A}\|}(\exp(\|\boldsymbol{A}\|(t - t_{is})) - 1) \qquad (51)
$$

which yields that the sampling interval $\Delta t_{i(s+1)} = t_{i(s+1)} - t_{is}$ satisfies

$$
\Delta t_{i(s+1)} \geq \frac{1}{\|\boldsymbol{A}\|}\ln\frac{\|\boldsymbol{A}\|\|\boldsymbol{e}_{iz}(t_{i(s+1)})\| + \beta_i + \|\boldsymbol{B}\|_{\mathrm{F}}\bar{u}_0}{\beta_i + \|\boldsymbol{B}\|_{\mathrm{F}}\bar{u}_0}.
$$

In what follows, the minimum sampling interval $\Delta t_{i,\min} = \min\{\Delta t_{is}\}_{s=1,2,...}$ is yielded as follow

$$
\Delta t_{i,\min} = \frac{1}{\|\boldsymbol{A}\|}\ln(\Psi_{i,\min} + 1) \qquad (52)
$$

with $\Psi_{i,\min}$ being the minimum value of $\Psi_i = \|\boldsymbol{A}\|\|\boldsymbol{e}_{iz}(t_{i(s+1)})\|/(\beta_i + \|\boldsymbol{B}\|_{\mathrm{F}}\bar{u}_0)$ for $t \in [t_{is}, t_{i(s+1)})$, $s \in \{0, 1, ...\}$. Obviously, we have $\Delta t_{i,\min} > 0$, which guarantees that Zeno behavior is excluded under the proposed triggering mechanism (22). The proof is completed. □

IV. Simulation Results

This section provides a simulation example to validate the proposed optimal event-triggered consensus method.

This article has been accepted for publication in IEEE Transactions on Automation Science and Engineering. This is the author's version which has not been fully edited and content may change prior to final publication. Citation information: DOI 10.1109/TASE.2026.3656938

A. Simulation Setup

Consider the MASs consisting of six follower agents and one leader agent, whose Laplacian matrix is presented by

$$\boldsymbol{\mathcal{L}} = \begin{bmatrix} 0 & 0 & 0 & 0 & 0 & 0 & 0 \\ -1 & 3 & -1 & 0 & 0 & 0 & -1 \\ 0 & -1 & 2 & -1 & 0 & 0 & 0 \\ 0 & 0 & -1 & 2 & -1 & 0 & 0 \\ 0 & 0 & 0 & -1 & 2 & -1 & 0 \\ 0 & 0 & 0 & 0 & -1 & 2 & -1 \\ 0 & -1 & 0 & 0 & 0 & -1 & 2 \end{bmatrix}.$$

The system matrices in [52] are selected as $\boldsymbol{A} = [\mathbf{0}_{3\times 3}, \boldsymbol{I}_3; \boldsymbol{A}_1, \boldsymbol{A}_2]$ and $\boldsymbol{B} = [\mathbf{0}_{3\times 3}; \boldsymbol{I}_3]$ with $\boldsymbol{A}_1 = [0, 0, 0; 0, 3 * 0.001^2, 0; 0, 0, -0.001^2]$ and $\boldsymbol{A}_2 = [0, 0.002, 0; -0.002, 0, 0; 0, 0, 0]$. The initial states of leader and follower agents are set as $\boldsymbol{x}_0(0) = \text{col}(0, 0, 0, 0)$, $\boldsymbol{x}_1(0) = \text{col}(0, 5, 2, 0, 0, 0)$, $\boldsymbol{x}_2(0) = \text{col}(-2, 2, 1, 0, 0, 0)$, $\boldsymbol{x}_3(0) = \text{col}(-3, -3, 1, 0, 0, 0)$, $\boldsymbol{x}_4(0) = \text{col}(1, -5, -1, 0, 0, 0)$, $\boldsymbol{x}_5(0) = \text{col}(-3, -3, 3, 0, 0, 0)$, and $\boldsymbol{x}_6(0) = \text{col}(4, 3, -2, 0, 0, 0)$. Other parameters are set as $\boldsymbol{u}_0 = 0$, $\boldsymbol{Q}_i = \boldsymbol{I}_4$, $\boldsymbol{R}_i = \boldsymbol{I}_2$, $\mu_i = 5$, and $\alpha_i = 2$ for $i \in \mathbb{I}_{[1:6]}$.

B. Effectiveness Validations

Under the conduction of the developed method and simulation setting of subsection IV-A, simulation results are plotted in Figs. 1-5. In particular, Fig. 1 depicts the trajectories of event-based local errors z_{i1s}, z_{i2s}, z_{i3s}, and z_{i4s} for $i \in \mathbb{I}_{[1:6]}$, which shows that the consensus of all follower agents is achieved. In Fig. 2, the sampling optimal policies u^*_{i1s} and u^*_{i2s} are depicted. Fig. 3 depicts the sampling interval of each follower agent from the current triggering time to the previous triggering one. In Fig. 4, two terms of the triggering function $\hbar(\boldsymbol{e}_{is}, \nabla V_i(\boldsymbol{z}_i))$ for $i \in \mathbb{I}_{[1:6]}$ are drawn to show the triggering conditions. Fig. 5 presents the sampling count curves of all agents. The triggering ratios relative to the total count of continuous sampling of each agent is calculated and recorded in TABLE I. Moreover, TABLE I also lists the maximum sampling intervals of each agent in Fig. 3 and triggering counts in Fig. 4. It is found that the developed event-triggered mechanism (22) ensure no Zeno behavior.

TABLE I: The maximum sampling interval, triggering count, and triggering ratio.

Agent	Maximum Interval	Triggering Count	Triggering Ratio
1	0.86s	148	7.40%
2	0.99s	158	7.90%
3	1.18s	101	5.05%
4	1.05s	104	5.20%
5	1.02s	99	4.95%
6	1.26s	89	4.45%

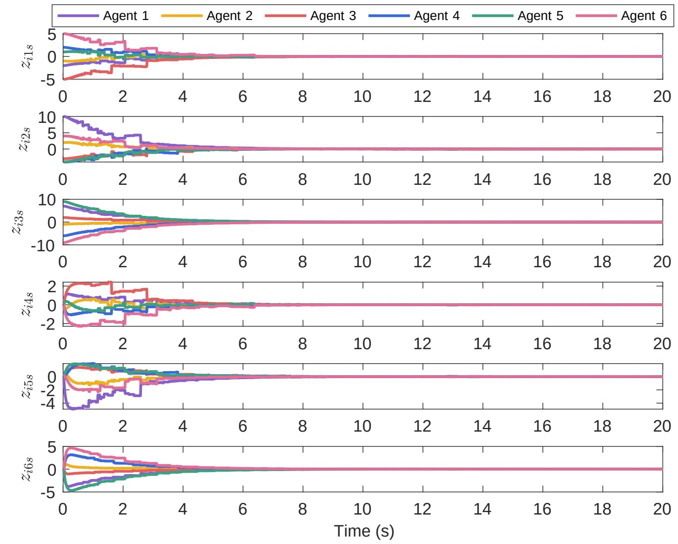

Fig. 1: Evolutions of event-based local errors of all agents.

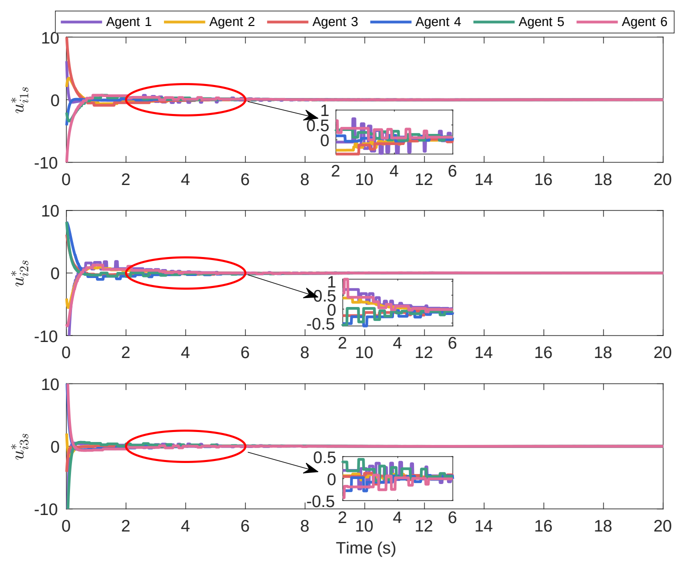

Fig. 2: The sampling inputs of all agents.

V. Conclusion

This paper investigates a game-based optimal event-triggered consensus method for MASs. Specifically, in the zero-sum game framework, a trade-off scheme between the performance index and sampling frequency is presented, where the optimal sampling interval can not only save communication resources but also minimize the corresponding performance index. Based on the differential graphical game theory, the optimal control law can drive neighboring agents to achieve the global Nash equilibrium with the information exchanges under the optimal event-triggered mechanism. Moreover, the designed optimal event-triggered mechanism can exclude the Zeno behavior by guaranteeing the positive minimum inter-event interval. Simulation results illustrated the effectiveness of the proposed optimal event-triggered consensus control method. Future works will take into consideration optimal event/self-triggered consensus problem of practical systems.

References

[1] V. Cichella, I. Kaminer, V. Dobrokhodov, E. Xargay, R. Choe, N. Hovakimyan, A. P. Aguiar, and A. M. Pascoal, "Cooperative path following

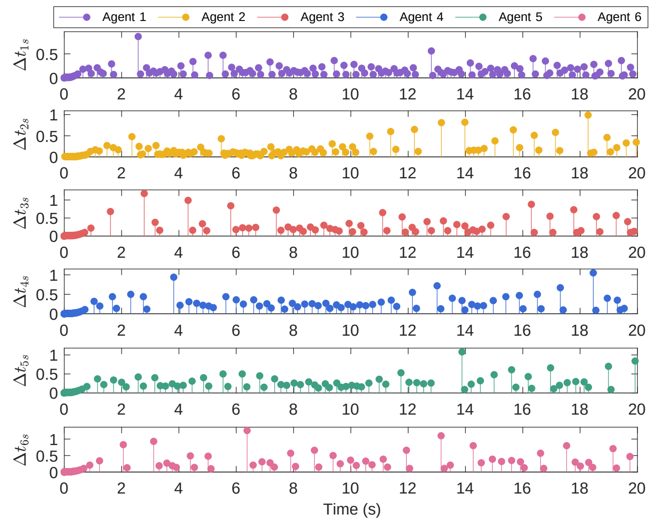

Fig. 3: The sampling intervals of agents 1 to 6.

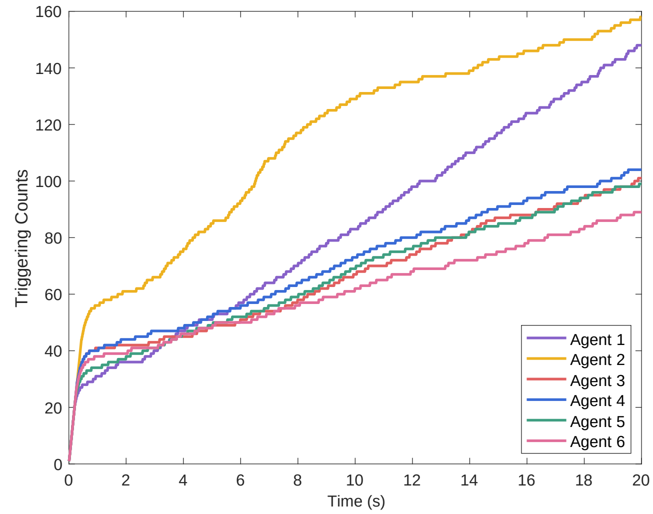

Fig. 5: The triggering counts of agents 1 to 6.

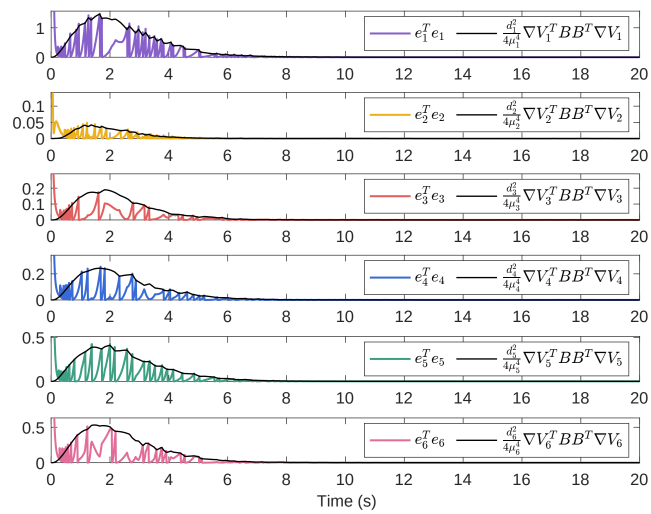

Fig. 4: The input sampling errors and triggering thresholds.

of multiple multirotors over time-varying networks," *IEEE Trans. Autom. Sci. Eng.*, vol. 12, no. 3, pp. 945–957, 2015.

[2] Y. Shi, C. Shen, H. Fang, and H. Li, "Advanced control in marine mechatronic systems: A survey," *IEEE/ASME Trans. Mechatron.*, vol. 22, no. 3, pp. 1121–1131, 2017.

[3] X. Dong, Y. Hua, Y. Zhou, Z. Ren, and Y. Zhong, "Theory and experiment on formation-containment control of multiple multirotor unmanned aerial vehicle systems," *IEEE Trans. Autom. Sci. Eng.*, vol. 16, no. 1, pp. 229–240, 2018.

[4] Y. Yu, C. Guo, and H. Yu, "Finite-time PLOS-based integral sliding-mode adaptive neural path following for unmanned surface vessels with unknown dynamics and disturbances," *IEEE Trans. Autom. Sci. Eng.*, vol. 16, no. 4, pp. 1500–1511, 2019.

[5] Z. Peng, J. Wang, D. Wang, and Q.-L. Han, "An overview of recent advances in coordinated control of multiple autonomous surface vehicles," *IEEE Trans. Ind. Informat.*, vol. 17, no. 2, pp. 732–745, 2021.

[6] X. Wang, S. Mou, and B. D. O. Anderson, "Consensus-based distributed optimization enhanced by integral feedback," *IEEE Trans. Autom. Control*, vol. 68, no. 3, pp. 1894–1901, 2023.

[7] C. Deng, L. Xu, T. Yang, D. Yue, and T. Chai, "Distributed cooperative optimization for nonlinear heterogeneous MASs under intermittent communication," *IEEE Trans. Autom. Control*, vol. 69, no. 4, pp. 2737–2744, 2024.

[8] J. Qin, Y. Wan, X. Yu, F. Li, and C. Li, "Consensus-based distributed coordination between economic dispatch and demand response," *IEEE Trans. Smart Grid*, vol. 10, no. 4, pp. 3709–3719, 2019.

[9] S. A. Alavi, K. Mehran, V. Vahidinasab, and J. P. S. Catalão, "Forecast-based consensus control for DC microgrids using distributed long short-term memory deep learning models," *IEEE Trans. Smart Grid*, vol. 12, no. 5, pp. 3718–3730, 2021.

[10] M. Mazo and P. Tabuada, "Decentralized event-triggered control over wireless sensor/actuator networks," *IEEE Trans. Autom. Control*, vol. 56, no. 10, pp. 2456–2461, 2011.

[11] H. Wang, N. Zhang, X. Liu, Y. Zou, and M. Li, "A simple event-based average consensus clock synchronization scheme in industrial wireless sensor networks under communication delays," *IEEE Trans. Ind. Informat.*, vol. 20, no. 8, pp. 10 113–10 122, 2024.

[12] X. Ge, Q.-L. Han, J. Wang, and X.-M. Zhang, "Scalable and resilient platooning control of cooperative automated vehicles," *IEEE Trans. Veh. Technol.*, vol. 71, no. 4, pp. 3595–3608, 2022.

[13] W. Wu, Y. Zhang, W. Zhang, R. Ji, and H. Chen, "Saturation-tolerant tunnel prescribed control for vessel-train formation of underactuated msvs," *IEEE Trans. Veh. Technol.*, vol. 73, no. 12, pp. 18 380–18 390, 2024.

[14] C. Zhao, J. He, P. Cheng, and J. Chen, "Consensus-based energy management in smart grid with transmission losses and directed communication," *IEEE Trans. Smart Grid*, vol. 8, no. 5, pp. 2049–2061, 2017.

[15] I. Ahmed, M. Rehan, N. Iqbal, and C. K. Ahn, "A novel event-triggered consensus approach for generic linear multi-agents under heterogeneous sector-restricted input nonlinearities," *IEEE Trans. Netw. Sci. Eng.*, vol. 10, no. 3, pp. 1648–1658, 2023.

[16] W. Wu, Z. Peng, L. Liu, and D. Wang, "A general safety-certified cooperative control architecture for interconnected intelligent surface vehicles with applications to vessel train," *IEEE Trans. Intell. Veh.*, vol. 7, no. 3, pp. 627–637, 2022.

[17] B. Ning, Q.-L. Han, and Q. Lu, "Fixed-time leader-following consensus for multiple wheeled mobile robots," *IEEE Trans. Cybern.*, vol. 50, no. 10, pp. 4381–4392, 2019.

[18] S. Wang and J. Huang, "Adaptive leader-following consensus for multiple Euler–lagrange systems with an uncertain leader system," *IEEE Trans. Neural Netw. Learn. Syst.*, vol. 30, no. 7, pp. 2188–2196, 2018.

[19] W. Wu, Y. Zhang, W. Zhang, and W. Xie, "Distributed finite-time performance-prescribed time-varying formation control of autonomous surface vehicles with saturated inputs," *Ocean Eng.*, vol. 266, 2022, doi:10.1016/j.oceaneng.2022.112866.

[20] W. Wang, Y. Li, and S. Tong, "Exact-optimal consensus of uncertain nonlinear multi-agent systems based on fuzzy approximation," *IEEE Trans. Autom. Sci. Eng.*, vol. 22, pp. 1497–1507, 2025.

[21] W. Wu, Y. Zhang, Z. Li, J.-G. Lu, and W. Zhang, "Constrained safe cooperative maneuvering of autonomous surface vehicles: A control barrier function approach," *IEEE Trans. Syst. Man, Cybern., Syst.*, vol. 55, no. 1, pp. 73–84, 2025.

[22] K. H. Movric and F. L. Lewis, "Cooperative optimal control for multi-agent systems on directed graph topologies," *IEEE Trans. Autom. Control*, vol. 59, no. 3, pp. 769–774, 2014.

This article has been accepted for publication in IEEE Transactions on Automation Science and Engineering. This is the author's version which has not been fully edited and content may change prior to final publication. Citation information: DOI 10.1109/TASE.2026.3656938

[23] T. Feng, H. Zhang, Y. Luo, and H. Liang, "Globally optimal distributed cooperative control for general linear multi-agent systems," *Neurocomputing*, vol. 203, pp. 12–21, 2016.

[24] T. Yang, Y. Wan, H. Wang, and Z. Lin, "Global optimal consensus for discrete-time multi-agent systems with bounded controls," *Automatica*, vol. 97, pp. 182–185, 2018.

[25] B. Mu and Y. Shi, "Distributed lqr consensus control for heterogeneous multiagent systems: Theory and experiments," *IEEE/ASME Trans. Mechatron.*, vol. 23, no. 1, pp. 434–443, 2018.

[26] H. Zhang, D. Yue, C. Dou, W. Zhao, and X. Xie, "Data-driven distributed optimal consensus control for unknown multiagent systems with input-delay," *IEEE Trans. Cybern.*, vol. 49, no. 6, pp. 2095–2105, 2019.

[27] Q. Wang, Z. Duan, Y. Lv, Q. Wang, and G. Chen, "Linear quadratic optimal consensus of discrete-time multi-agent systems with optimal steady state: A distributed model predictive control approach," *Automatica*, vol. 127, p. 109505, 2021.

[28] Y. Ren, Q. Wang, and Z. Duan, "Optimal distributed leader-following consensus of linear multi-agent systems: A dynamic average consensus-based approach," *IEEE Trans. Circuits Syst. II Express Briefs*, vol. 69, no. 3, pp. 1208–1212, 2021.

[29] L. Ding, Q. Han, X. Ge, and X. Zhang, "An overview of recent advances in event-triggered consensus of multiagent systems," *IEEE Trans. Cybern.*, vol. 48, no. 4, pp. 1110–1123, 2018.

[30] X. Ge, Q.-L. Han, X.-M. Zhang, L. Ding, and F. Yang, "Distributed event-triggered estimation over sensor networks: A survey," *IEEE Trans. Cybern.*, vol. 50, no. 3, pp. 1306–1320, 2020.

[31] P. Tabuada, "Event-triggered real-time scheduling of stabilizing control tasks," *IEEE Trans. Autom. control*, vol. 52, no. 9, pp. 1680–1685, 2007.

[32] G. S. Seyboth, D. V. Dimarogonas, and K. H. Johansson, "Event-based broadcasting for multi-agent average consensus," *Automatica*, vol. 49, no. 1, pp. 245–252, 2013.

[33] Y. Wu, H. Zhang, Z. Wang, and C. Huang, "Distributed event-triggered consensus of general linear multiagent systems under directed graphs," *IEEE Trans. Cybern.*, vol. 52, no. 1, pp. 608–619, 2020.

[34] Y.-Y. Qian, L. Liu, and G. Feng, "Output consensus of heterogeneous linear multi-agent systems with adaptive event-triggered control," *IEEE Trans. Autom. Control*, vol. 64, no. 6, pp. 2606–2613, 2018.

[35] X. Li, Y. Tang, and H. R. Karimi, "Consensus of multi-agent systems via fully distributed event-triggered control," *Automatica*, vol. 116, p. 108898, 2020.

[36] A. Girard, "Dynamic triggering mechanisms for event-triggered control," *IEEE Trans. Autom. Control*, vol. 60, no. 7, pp. 1992–1997, 2014.

[37] W. He, B. Xu, Q.-L. Han, and F. Qian, "Adaptive consensus control of linear multiagent systems with dynamic event-triggered strategies," *IEEE Trans. Cybern.*, vol. 50, no. 7, pp. 2996–3008, 2020.

[38] M. Li, Y. Long, T. Li, H. Liang, and C. L. P. Chen, "Dynamic event-triggered consensus control for input constrained multi-agent systems with a designable minimum inter-event time," *IEEE/CAA J. Autom. Sinica*, vol. 11, no. 3, pp. 649–660, 2024.

[39] T. Xu, Z. Duan, G. Wen, and Z. Sun, "A novel dynamic event-triggered mechanism for dynamic average consensus," *Automatica*, vol. 161, p. 111495, 2024.

[40] W. Xu, W. He, D. W. Ho, and J. Kurths, "Fully distributed observer-based consensus protocol: Adaptive dynamic event-triggered schemes," *Automatica*, vol. 139, p. 110188, 2022.

[41] B. Cheng and Z. Li, "Coordinated tracking control with asynchronous edge-based event-triggered communications," *IEEE Trans. Autom. Control*, vol. 64, no. 10, pp. 4321–4328, 2019.

[42] H. Zhao, X. Meng, and S. Wu, "Distributed edge-based event-triggered coordination control for multi-agent systems," *Automatica*, vol. 132, p. 109797, 2021.

[43] A. Sahoo, V. Narayanan, and S. Jagannathan, "A min–max approach to event-and self-triggered sampling and regulation of linear systems," *IEEE Trans. Ind. Electron.*, vol. 66, no. 7, pp. 5433–5440, 2018.

[44] W. Xu, T. Wang, J. Qiu, and X. Liu, "A novel framework for game-based optimal event-triggered control of multi-input nonlinear systems," *IEEE Trans. Autom. Control*, vol. 69, no. 7, pp. 4867–4874, 2024.

[45] W. Ren and R. W. Beard, *Distributed Consensus in Multi-Vehicle Cooperative Control*. Springer, 2008, vol. 27, no. 2.

[46] J. Zhao, C. Yang, W. Gao, and J. H. Park, "Novel single-loop policy iteration for linear zero-sum games," *Automatica*, vol. 163, p. 111551, 2024.

[47] B. Gharesifard and J. Cortés, "Distributed convergence to Nash equilibria in two-network zero-sum games," *Automatica*, vol. 49, no. 6, pp. 1683–1692, 2013.

[48] X. Liu, H. Yan, W. Zhou, N. Wang, and Y. Wang, "Event-triggered optimal tracking control for underactuated surface vessels via neural reinforcement learning," *IEEE Trans. Ind. Informat.*, vol. 20, no. 11, pp. 12 837–12 847, 2024.

[49] M. Abbasi and H. J. Marquez, "Observer-based event-triggered consensus control of multi-agent systems with time-varying communication delays," *IEEE Trans. Autom. Sci. Eng.*, vol. 21, no. 4, pp. 6336–6346, 2024.

[50] Y. Wu, M. Chen, M. Chadli, and H. Li, "Dual-type-triggers-based cooperative adaptive critic control of swarm UAVs under FDI attacks," *Automatica*, vol. 167, p. 111757, 2024.

[51] W. Wu, Z. Peng, D. Wang, L. Liu, and Q.-L. Han, "Network-based line-of-sight path tracking of underactuated unmanned surface vehicles with experiment results," *IEEE Trans. Cybern.*, vol. 52, no. 10, pp. 10 937–10 947, 2022.

[52] W. Hu, C. Yang, T. Huang, and W. Gui, "A distributed dynamic event-triggered control approach to consensus of linear multiagent systems with directed networks," *IEEE Trans. Cybern.*, vol. 50, no. 2, pp. 869–874, 2018.

[53] M. Abbasi and H. J. Marquez, "Dynamic event-triggered formation control of multi-agent systems with non-uniform time-varying communication delays," *IEEE Trans. Autom. Sci. Eng.*, vol. 22, pp. 8988–9000, 2025.

[54] Y.-S. Ma and W.-W. Che, "Fully distributed consensus control under dual-channel dynamic event-triggered strategies," *IEEE Trans. Autom. Sci. Eng.*, vol. 22, pp. 16 560–16 571, 2025.

[55] X. Li, Z. Sun, Y. Tang, and H. R. Karimi, "Adaptive event-triggered consensus of multiagent systems on directed graphs," *IEEE Trans. Autom. Control*, vol. 66, no. 4, pp. 1670–1685, 2021.

[56] Z. Xiao, Z. Xiao, J. Tao, C. Liu, P. Shi, and I. J. Rudas, "Adaptive event-triggered heterogeneous consensus of leader-following multi-agent systems with nonlinear dynamic topology," *IEEE Trans. Autom. Sci. Eng.*, vol. 22, pp. 5781–5791, 2025.

[57] H. K. Khalil, *Nonlinear Systems Third Edition*, 2002, vol. 115.

[58] K. G. Vamvoudakis, "Event-triggered optimal adaptive control algorithm for continuous-time nonlinear systems," *IEEE/CAA J. Autom. Sinica*, vol. 1, no. 3, pp. 282–293, 2014.

Wentao Wu (Member, IEEE) received the Ph.D. degree from Shanghai Jiao Tong University, Shanghai, China, 2025. From January to November 2024, he was a Visiting Research Scholar at the Department of Mechanical Engineering, University of Victoria, BC, Canada. He is currently a Postdoctoral Fellow in the Department of Aeronautical and Aviation Engineering, The Hong Kong Polytechnic University.

His current research interests include distributed control, safety-critical control, game theory, and their applications in marine vehicles. Dr. Wu was selected for the inaugural Doctoral Special Program of Young Elite Scientist Sponsorship Program by China Association for Science and Technology (CAST) in 2025. He serves as an active reviewer of many international journals.

Lei Xu (Member, IEEE) received the Ph.D. degree in mechanical engineering from the University of Victoria, Victoria, BC, Canada, in 2025. He is currently a Postdoctoral Researcher with the School of Electrical Engineering and Computer Science, KTH Royal Institute of Technology, Stockholm, Sweden.

His research interests include distributed optimization, networked control systems, event-triggered control, and Markovian jump systems.

Yibo Zhang (Member, IEEE) is currently an Associate Professor at the Department of Automation, Shanghai University,Shanghai, China. He received his B.E. degree in Marine Electronic and Electrical Engineering and Ph.D. degree in Marine Electrical Engineering from Dalian Maritime University, Dalian, China, in 2014 and 2021, respectively. From September 2021 to November 2024, he worked as a Postdoctoral Fellow in the Department of Automation, Shanghai Jiao Tong University, Shanghai, China.

His current research interests focus on the cooperative control and intelligent control of uncertain nonlinear systems, as well as multi-agent systems with applications in marine vehicles.

Weidong Zhang (Senior Member, IEEE) received his BS, MS, and PhD degrees from Zhejiang University, China, in 1990, 1993, and 1996, respectively, and then worked as a Postdoctoral Fellow at Shanghai Jiaotong University. He joined Shanghai Jiaotong University in 1998 as an Associate Professor and has been a Full Professor since 1999. From 2003 to 2004 he worked at the University of Stuttgart, Germany, as an Alexander von Humboldt Fellow. From 2007 to 2008 he worked at Princeton University, USA, as a Visiting Professor. From 2013 to 2017 he serviced as Deputy Dean of the Department of Automation, Shanghai Jiaotong University. He serving as a part-time professor at Hainan University from 2021. He is currently Chair Professor of Shanghai Jiaotong University, Director of the Engineering Research Center of Marine Automation, Shanghai Municipal Education Commission, China.

His research interests include control theory, machine learning theory, and their applications in industry and robots. He is the author of more than 300 papers and 2 books. His papers have been cited for more than 23k times in Google, and he is recognized as Elsevier Most Cited Researcher and Highly Ranked Scholar-Lifetime in the Specialties of Sensor fusion, Control theory by ScholarGPS.

Yang SHI (IEEE Fellow) received his B.Sc. and Ph.D. degrees in mechanical engineering and automatic control from Northwestern Polytechnical University, Xi'an, China, in 1994 and 1998, respectively, and the Ph.D. degree in electrical and computer engineering from the University of Alberta, Edmonton, AB, Canada, in 2005. He was a Research Associate in the Department of Automation, Tsinghua University, China, during 1998-2000. From 2005 to 2009, he was an Assistant Professor and Associate Professor in the Department of Mechanical Engineering, University of Saskatchewan, Saskatoon, SK, Canada. In 2009, he joined the University of Victoria, and now he is a Professor in the Department of Mechanical Engineering, University of Victoria, Victoria, BC, Canada. His current research interests include networked and distributed systems, model predictive control (MPC), cyber-physical systems (CPS), robotics and mechatronics, navigation and control of autonomous systems (AUV and UAV), and energy system applications.

On teaching and mentorship, Dr. Shi received the University of Saskatchewan Student Union Teaching Excellence Award in 2007, the Faculty of Engineering Teaching Excellence Award in 2012 at the University of Victoria (UVic), and the 2023 REACH Award for Excellence in Graduate Student Supervision and Mentorship. On research, he is the recipient of the JSPS Invitation Fellowship (short-term) in 2013, the UVic Craigdarroch Silver Medal for Excellence in Research in 2015, the Humboldt Research Fellowship for Experienced Researchers in 2018, CSME Mechatronics Medal (2023), IEEE Dr.-Ing. Eugene Mittelmann Achievement Award (2023), the 2024 IEEE Canada Outstanding Engineer Award. He was a Vice-President on Conference Activities of IEEE IES (2022-2025) and the Chair of IEEE IES Technical Committee on Industrial Cyber-Physical Systems. Currently, he is IFAC Council Member and Editor-in-Chief of IEEE Transactions on Industrial Electronics; he also serves as Associate Editor for Automatica, IEEE Transactions on Automatic Control, Annual Review in Controls, etc.

He is a Fellow of IEEE, ASME, CSME, Engineering Institute of Canada (EIC), Canadian Academy of Engineering (CAE), Royal Society of Canada (RSC), and a registered Professional Engineer in British Columbia, Canada.